Lawrence Berkeley Laboratory
UNIVERSITY OF CALIFORNIA

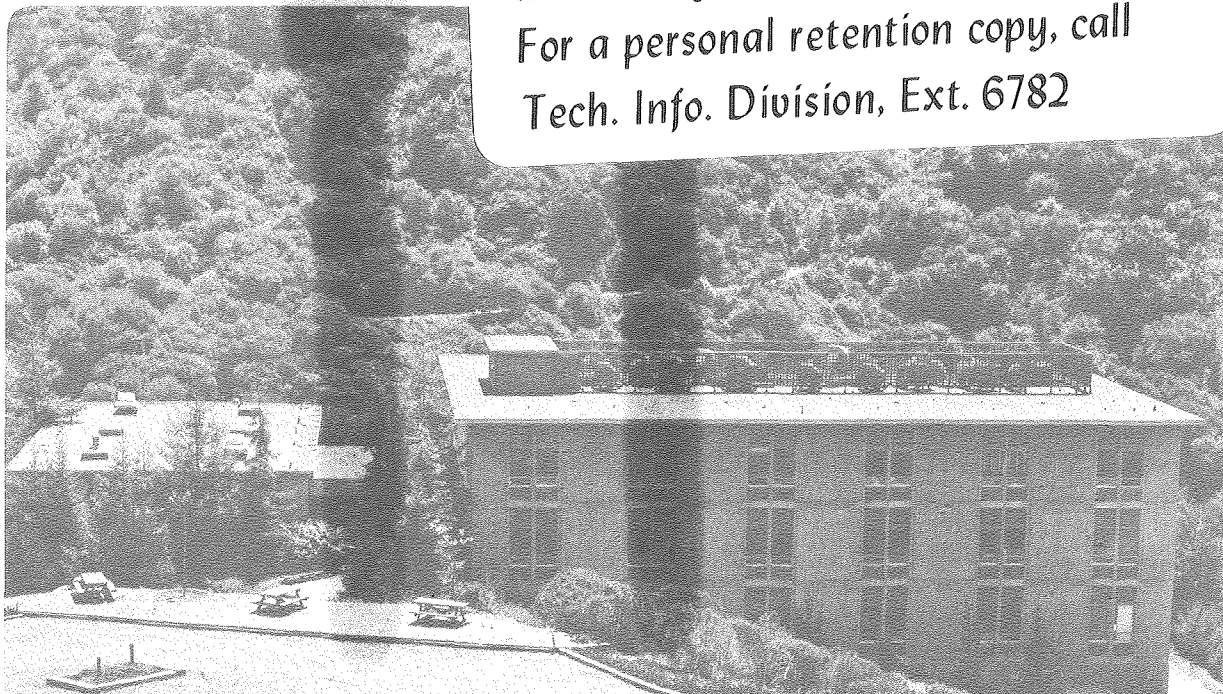## Materials & Molecular Research Division

ELECTROCHEMICAL STUDIES OF THE FILM FORMATION ON LITHIUM IN PROPYLENE CARBONATE SOLUTIONS UNDER OPEN CIRCUIT CONDITIONS

Y. Geronov, F. Schwager, and R.H. Muller

April 1981

DISCLAIMER

Electrochemical Studies of the Film Formation

on Lithium in Propylene Carbonate

Solutions under Open Circuit Conditions

Y. Geronov*, F. Schwager and R. H. Muller

Materials and Molecular Research Division
Lawrence Berkeley Laboratory
University of California
Berkeley, CA 94720

Abstract

The nature of protective surface layers formed on lithium in

propylene carbonate solutions of $LiClO_4$ and $LiAsF_6$ at open circuit

has been investigated by electrochemical pulse measurements and

other techniques. The results are consistent with the fast formation

of a compact thin layer of Li_2O by reaction with residual water.

This layer acts as a solid ionic conductor. Slow corrosion processes

produce a thicker porous overlayer.

---

*Permanent address: Central Laboratory of Electrochemical Power Sources,
                     Bulgarian Academy of Sciences, Sofia, Bulgaria.

Lithium is thermodynamically unstable in contact with most nonaqueous battery electrolytes and can be used only because of the formation of protective films on the metal. In a review paper[1] Dey has pointed out the importance of surface layers for battery performance and shown scanning electron microscope (SEM) pictures of anode surfaces after reaction under different conditions. In more recent papers by Peled[2,3] the effect of passivating films on electrode kinetic parameters has been shown. It is now generally assumed[2-5] that in most cases the rate-determining step (rds) of the dissolution-deposition process of alkali metals in nonaqueous solutions is not electron charge transfer but the migration of cation lattice defects through the surface layer.

Up to now the main effort of investigation of passivity of lithium has dealt with $Li/SOCl_2$ batteries where the "voltage delay" problem is very significant. Studies of the formation of passivating films on Li in propylene carbonate (PC) solutions have been initiated more recently. Their properties have been shown to affect the cycling efficiency of secondary Li electrodes[6,7]. Alloying with an aluminum substrate has been found beneficial[8]. Attempts have been made by Dey[1] to examine the morphology of Li films in PC using SEM. His conclusion was that a film of Li_2CO_3 "appears to be extremely thin". The same author, as well as Peled[3], have used the previous data of Scarr[9] dealing with the dual Tafel behavior of Li in PC solutions, in order to support their assumption of the existence of a surface layer and its influence on the electrode kinetics. Scarr has analyzed his experimental results by means of the Butler-Volmer equation.

The aim of this study is to investigate the kinetics of film formation on lithium in propylene carbonate solutions with different solutes and to determine some film characteristics such as resistence, conductivity and thickness.

Two principal ways of investigating these problems were chosen: electrochemical - by using galvanostatic pulse techniques and ellipsometry. This paper is mainly dealing with electrochemical measurements while the results from the ellipsometry will be presented separately. The basic assumption of this study is that lithium in PC is covered by a dense surface layer. It had been suggested before[3] that this layer is formed instantly by the contact of the metal with the solution. It is found here to continue to grow with time. The layer consists of some insoluble products of the reaction of lithium with propylene carbonate, such as Li_2CO_3, with water, such as $LiOH$ or Li_2O, or another constituent of the solution. It acts as a Li conducting solid electrolyte[6] with no electronic conductivity and has been called Solid Electrolyte Interphase (SEI)[3]. The capacitance across this film is assumed to be electrically connected in series with that of the electrolytic double layer.

The electrochemical behavior of SEI electrodes will be governed by the properties of the SEI. When the SEI is thick enough the migration of ions through it may be the rate-determining step. In this case it is possible to use the basic equation of the classical theory of ionic conduction in solids developed by Frenkel, Varwey, Cabrera and Mott, and Young[10]:

$$i = 4q\nu \; Fan_+ \; exp \; (-W/RT) \; sinh \; (aqFE/RT), \qquad (1)$$

where i is the current density, q the charge of the mobile ion, ν the vibration frequency, W the barrier energy, a the half-jump distance and E the electric field strength. At higher electric fields Eq.(1) can be simplified to:

$$i = i_0 \; exp \; (BE) = i_0 \; exp \; (B\frac{\eta}{Y}), \qquad (2)$$

where i_0 is the zero-field ionic current density, B is the field coefficient, η is the potential difference across the film, and Y is the film thickness. Equation (2) represents a Tafel-like polarization dependence.

From this equation a Tafel slope, b, which increases with the film thickness is obtained:

$$b = 2.3 \frac{Y}{B} . \tag{3}$$

For low field conditions, Eq. (1) reduces to Ohm's law:

$$i = \kappa \frac{\eta}{Y} , \tag{4}$$

where κ is the specific conductivity of the SEI. The reaction resistance R_p of an electrode is defined as:

$$R_p = (\frac{\eta}{i})_{\eta \to 0} . \tag{5}$$

Thus:

$$R_p = \frac{1}{\kappa} \times Y . \tag{6}$$

From Eq.(1), for the limiting case when the field strength tends to be zero, one obtains:

$$(i)_{E=0} = i_0 B E \tag{7}$$

At low fields, as has been shown, Ohm's law is applicable and hence:

$$\kappa = (\partial i / \partial E)_{E=0} = i_0 B, \tag{8}$$

where i_0 is the extrapolated zero-field ionic current density.

Experimental

An electrochemical cell was built to make simultaneous electrochemical and ellipsometric measurements in situ. Clean, optically smooth lithium electrodes were prepared and inserted into the cell in inert atmosphere by pressing 3 mm thick, 5 cm^2 round lithium discs (Foote Mineral, high purity, scraped with a blade) on a polycarbonate foil (cleaned with hexane, alcohol, boiling water (1h), steam (2-3h) and dried in vacuum at 90-100°C) in a special jig. The cross-section of a 3.2 mm diam. freshly extruded Li wire, positioned 1 mm from the periphery of the test electrode, served as reference electrode.

Two types of solutions were used:

(a) propylene carbonate - $LiClO_4$

(b) propylene carbonate - $LiAsF_6$

Propylene carbonate (Burdick & Jackson, Muskegon, MI. 49442; distilled in glass) was distilled in a low-pressure distillation column under He atmosphere. The reflux ratio was between 60 and 100 and the head temperature was 145°C. Gas chromatographic analysis showed the water content to be always below 50 ppm. $LiClO_4$ (Alfa p.a.) was dried under vacuum (4-5 mm Hg) at 220°C for 48-73 hours. $LiAsF_6$ (Alfa p.a.) was dried under vacuum at ambient temperature for 7-8 days.

The solutions with 0.05 and 0.1% H_2O were prepared by adding water into PC. The solutes were dissolved in the above solutions. In order to avoid any possible reaction of PC vapor with the lithium surface before contact with the liquid, different glove boxes were used for the preparation of electrodes and solutions.

The delay in electrochemical measurements from the moment of electrode scraping was up to 30-45 minutes; the delay after electrolyte filling was 15-30 seconds. Film formation under open circuit conditions was followed by periodic determinations of electrode capacitance and polarization resistance $R_p = (\partial \eta / \partial i)_{\eta=0}$ by means of the galvanostatic pulse polarization technique. The transients were recorded with a Tektronix 5111 storage oscilloscope, equipped with a Tektronix C-50 camera. A 214B Hewlet Packard pulse generator was used either through a high resistance or through a potentionstat with 2 μs rise time (PAR-371).

The capacitance was derived from the initial slope of short η-t transients (5-10 μs) (Fig. 1a). Anodic and cathodic pulses produced the same results. The steady-state IR-free overpotential values for the determination of R_p were obtained from oscilloscopic traces with a duration of up to 20 ms. (Fig. 1b). To avoid damage to the film, pulses with the smallest possible electric charge were applied.

Results and Discussions

1. Film Thickness

The thickness Y of the film formed during the contact of the lithium elec-

trode with propylene carbonate solutions has been derived from the capacitance measurements by use of the formula for two capacitors connected in series[3,4]

$$Y = \frac{\sigma \varepsilon}{0.113C} - Y' \, \varepsilon/\varepsilon' \; [\text{Å}] \qquad\qquad (9)$$

where ε is the dielectric constant of the lithium film $\varepsilon' = 65$ that of PC, C is the capacitance of the electrode in $\mu F/cm^2$, and σ is the roughness factor, which is assumed to be unity. Dielectric constants of materials of interest here are listed in Table 1. The thickness Y' of the Helmholz layer in concentrated electrolytes can be approximated by the length of the dipole (ca. 5 Å for PC); the second right hand term in Eq. (9) can therefore be neglected. In order for Eq. (9) to be used correctly, two questions should be answered: (a) what is the film dielectric constant, and (b) what is the film morphology - nonporous, porous or both.

(a) Dielectric Constant of Film Material

There are a lot of controversial opinions about the film composition on lithium in PC electrolytes. According to Dey[1], Dousek et al.[11] PC reacts with Li forming Li_2CO_3. On the other hand Butler et al.[12] have demonstrated the predominant role of small amounts of water in the kinetics of fresh Li surfaces. Dousek et al. have pointed out the lack of any decomposition reaction on the bulk Li surface and even a drastically decreasing rate of PC decomposition on Li amalgam at only 45 ppm H_2O in the PC-LiClO$_4$ solution. Recently, Epelboin et al.[13] by ESCA analysis have claimed that PC leads to a chemical formation of a polymeric membrane on the Li substrate.

In this investigation the composition of the passive film formed on Li from different PC solutions was examined by Auger spectroscopy and the results will be discussed later (See paragraph 6). For the calculation of film thickness a dielectric constant of 5 was used. This value is close to that of both Li_2CO_3 and LiOH[14,15]. But one should keep in mind that for example at $\varepsilon = 10$ the film thickness will double which in general does not change the presented considerations.

(b) Morphology of Film

Recently it was shown[16] that the primary passive film on Li, found in $SOCl_2$ - $LiAlCl_4$ solutions is dense and porefree. In order to answer this question for propylene carbonate solutions a Li electrode was kept for 120 hours in pure solvent. After that the PC was changed sequentially by two solutions 0.15M $LiClO_4$/PC and 1.0M $LiClO_4$/PC. The electrode capacitance and resistance have been measured for 24 hours in each solution. No change of the electrode capacitance or the polarization resistance was detected. Their values remain the same during two days: $C = 0.14 \pm 0.02$ $\mu F/cm^2$ and $R_p = 380 \pm 20$ ohm cm^2. The constancy of the film resistance R_p when the electrolyte concentration was changed approximately one order of magnitude yields strong evidence for a dense passive film on lithium in propylene carbonate.

As will be shown further the higher water amounts in the PC solutions increase a probability of a secondary porous film formation. The porous film does not possess protective properties and presumably would influence to a negligible extent the passive behavior of lithium in PC solutions, since the passivity of Li is governed by the primary nonporous film. Data for the primary passive film measured after up to 4-5 days storage were considered more accurate because the porous film is not yet very thick or dense.

2. High-Field Experiments

The steady-state iR-free overpotential values were calculated from the transients in the range of current densities between 0.050-20 mA/cm^2 (see Fig. 1b). At the higher current densities (i.e. higher electric fields, above about 10^6 V/cm), a Tafel-like polarization dependence is expected (Eq.2). Figure 2 presents a series of Tafel plots, obtained by the pulse technique for different film thicknesses. As required for a field-assisted ion current across an insulating film, the Tafel slope, b, increases with film thickness. The extrapolated lines intersect at zero overpotential at the zero field c.d., $i_0 = 3$ mA/cm^2.

Curve 1 of Figure 2 was obtained a few minutes after electrolyte filling. The value of the zero-field current density i_o of 5.5 mA/cm^2 obtained by this plot can be compared to exchange currents reported by other authors in terms of the electron transfer reaction mechanism. For example, Butler, et al.[12] have reported an extrapolated value of the exchange current in 0.001M H$_2$O/PC/ LiClO$_4$ on freshly cut Li surface of 12 mA/cm^2. An exchange current of 3.3 mA/cm^2 was reported by Epelboin et al.[13] by using anodic polarization techniques for surface cleaning. The value of 5.5 mA/cm^2 obtained in this study for the specularly reflecting Li surface coincides well with the value of 12 mA/cm^{2}[12] for a roughness factor of 2 to 3 given by the previous authors[13]. This is evidence for comparable cleanliness of the Li surfaces used in both studies.

This higher value of i_o obtained just after immersing the electrode as compared to the zero field current (2.7-3.0 mA/cm^2) leads to the following suggestions:

(a) In the very beginning after electrode immersion in the solution, the electrode charge transfer step is the determining rate.

(b) The existence of a thin film layer different from the passivating layer, formed in the solution. The space-charge can also influence the kinetics of ion migration in solids at thinner films.

The low electrode capacitance of 1.3-1.6 μF/cm^2 assessed in this study supports the last assumption giving film thicknesses of 15-25 Å for ϵ = 5-10.

The value of the field coefficient B (Eq. 3) may be obtained from the slope b-Y, presented in Fig. 3. This value, B = 1.2 $\pm$ 0.1 x 10^{-6} cm/V is very close to that of typical barrier films.[10]

The data in Fig. 2 are presented as the plots of log i - E (Curve 2) in Fig. 4. It is found that the current density does not depend on the film thickness which supports the assumption of the rate determining step being the ion migration through the film. From the plot log i - E, using Eq. (2) the value of B can be determined once more. In the same Fig. 4, the Tafel plots

of Li in PC/0.5M LiAsF$_6$ and in PC/0.5M LiClO$_4$ + 0.1% H$_2$O are presented in comparison. It can be seen that the field coefficient, B, (slope, Eq. 2) is lower in water-contaminated PC/LiClO$_4$ solutions but it increases in PC/LiAsF$_6$ solutions (1.8 $\pm$ 0.1 x 10^{-6} cm/V).

However, the zero-field current density remains the same (2.9 $\pm$ 0.2 x 10^{-3} A/cm^2). This indicates similar film properties in different media. These values of B and i$_o$ were used to calculate the specific conductivity of the film by the low-field approximation Eq. (8), namely (3.1 $\pm$ 0.25) x 10^{-9} ohm^{-1} cm^{-1} for LiClO$_4$ solutions and (5.1 $\pm$ 0.2) x 10^{-9} ohm^{-1} cm^{-1} for LiAsF$_6$ solutions.

The experimentally found values of the Tafel slope, b, at different film thicknesses can be derived from Fig. 2 . As has been seen from Eqs. (1-3), the Tafel slope is equal to:

$$b = \frac{2.3 \; RT \; Y}{aqF} \; . \tag{10}$$

For q = 1 and a = 3 Å this formula is simplified to:

$$b(mv) = 20Y \; . \tag{11}$$

A comparison between the experimental and theoretical values of b is given in Table II. If one considers that other combinations of dielectric constant ε and half-jump distance a of the film could be used, the agreement of measured and computed Tafel slopes (for ε = 5 and a = 3 Å) is satisfactory.

3. Low Field Experiments

Figures 5 and 6 present typical sets of experimental plots reflecting the increase of the electrode resistance R$_p$ and the reciprocal capacitance 1/C with time for Li electrodes immersed in PC/LiClO$_4$ and PC/LiAsF$_6$ solutions respectively. It was found in more than 30 experimental cells that all 1/C - R plots meet the same point with the coordinates: 1/C = 0.70 $\pm$ 0.10 cm^2/μF and R = 8 $\pm$ 2 ohm cm^2.

This suggests the existence of a capacitance connected in series with the capacitance across the passive film. This capacitance is low compared to that of the Helmholz double layer (10-20 μF/cm^2 [8, 12, 13]) and probably it is a

capacitance of the lithium oxide (hydroxide) formed in the glove box[17] (See the previous paragraph).

Hence the thickness of the film formed during the contact of lithium with the solution can be calculated from Eq. (12); instead of Eq. (9):

$$Y = 8.85 \times 10^{-8} \ \varepsilon\sigma \ (1/C - 1/C_d) \ [cm] \tag{12}$$

where C is the film capacitance and C_d is the intersection of the plot $(1/C - R_p)$ with the 1/C ordinate (actually this involves an error of a few Å if instead of R_p = 5 - 8 ohm cm^2, R_p = 20 is taken).

From the slope of $1/C - R_p$, using Eq. (6) and (12), the values of specific conductivity of the primary passive film in different PC solutions can be derived. This value for PC/LiClO$_4$ solutions is $2.7 \pm 0.2 \times 10^{-9}$ ohm^{-1} cm^{-1} (Fig. 5) and for PC/LiAsF$_6$ - $5.1 \pm 0.25 \times 10^{-9}$ ohm^{-1} cm^{-1} (Fig. 6). Both are very close to the value of κ, estimated from the low-field approximation formula (8) (See Fig. 2-4).

4. Effect of Water

Fig. 7 presents the change of the electrode resistance during the time of storage. In the same figure, curve 1 and 2 are for 0.5M LiAsF$_6$ solutions with 20 and 1000 ppm H$_2$O respectively and curves 3, 4 and 5 are for 0.5M LiClO$_4$ solutions with 20,500 and 1000 ppm H$_2$O respectively. The curves show that the rate of film formation increases with water concentration. This trend is much stronger in PC/LiClO$_4$ solutions than in LiAsF$_6$.

From Fig. 6 it also can be seen that there is no difference between the conductivity of film formed in PC/0.5M LiAsF$_6$ with 20 ppm H$_2$O and those with 1000 ppm H$_2$O. On the other hand, the film conductivity in LiAsF$_6$ solutions is always higher than in LiClO$_4$ solutions independent from the water concentration. For example, from Fig. 5, curves 2 and 3, the calculated values of κ in LiClO$_4$ solutions with 500-1000 ppm H$_2$O are 0.8 to 1.5×10^{-9} cm^{-1} ohm^{-1}, which is approximately 4-7 times lower than in LiAsF$_6$ solutions (Fig. 6). The former

values are 2-3 times lower than the conductivity of passive films formed in
$LiClO_4$ solutions with 20 ppm H_2O ($2.5 - 3.5 \times 10^{-9}$ ohm^{-1} cm^{-1}).

The same tendency of thin film conductivity change is also demonstrated
from the high-field experiments (see Fig. 4) but to a lesser extent. For example,
the expected field coefficient, B, for PC/0.5M $LiClO_4$ solutions with 1000 ppm
of water should be approximately 2 times lower in order to fit the calculated
value of specific conductivity according to Eq. (8) ($\kappa = i_0 B$) to that obtained
from low field experiments (Fig. 5). This disagreement, found only in PC/$LiClO_4$
solution of high water content is probably due to some influence of the second-
ary porous film. On the other hand it is noteworthy that the Tafel plots log
i - E taken from the passivated lithium electrode in pure PC, PC with 0.5M
$LiAsF_6$ and PC/$LiAsF_6$ with 1000 ppm H_2O show the same slope, the same field
coefficient B = 1.8×10^{-6} V^{-1} cm, and zero current density i_0 = 2.7×10^{-3} A/cm^2
(Fig. 8). The specific conductivity calculated using these values of B and i_0
is very close to the one found for $LiAsF_6$ solutions from low field experiments
(see Fig. 6), 4.9×10^{-9} ohm^{-1} cm^{-1}.

This observation support the following ideas: (a) passive layers are
formed the same way in PC without any salt and with $LiAsF_6$ as solute; (b) $LiAsF_6$
does not take part in the film formation; (c) film is formed as a result of
reaction of Li with water impurity. The last suggestion is reinforced by the
increase of rate formation with water concentration.

A very surprising result from this set of experiments was that lithium
corroded faster in PC (without salt) containing 0.1% H_2O than in solutions of
$LiClO_4$ and $LiAsF_6$ with the same amount of water. After 7 days storage in this
solution a lithium mirror-like bright surface turns to complete dark gray. This
has never happened in the solutions with $LiClO_4$ or $LiAsF_6$ with the same water
concentrations. Electron micrographs presented below also illustrate this
difference. This opens another point of consideration, the possible interaction
between water and solutes. As a result, the water activity involved in the

direct reaction with lithium could be reduced. However, special spectroscopic investigations would be necessarily to elucidate this problem.

So far, there is no reasonable explanation for the decrease in film conductivity with increasing water content of $LiClO_4$ solutions. However, the fact that even in $LiClO_4$ solutions with low H_2O concentration the film conductivity is always lower than in $LiAsF_6$ solutions and pure PC suggests the important role of $LiClO_4$ in the film formation. This is also supported from SEM pictures showing in $PC/LiClO_4$ solution a different microstructure from this in pure PC and $PC/LiAsF_6$.

5. Effect of Cathodic Pulse Polarizations

It was found that an asymmetric overpotential behavior of the Li electrode in $PC/LiClO_4$ solutions occurs under anodic and cathodic galvanostatic pulses. Figure 9 presents the relationship between $\Delta\eta$ and film thickness at 0.5 mA/cm^2 and 1 mA/cm^2 current pulses of 10 ms duration. $\Delta\eta$ is defined as the difference between cathodic and anodic overpotentials free of ohmic drop.

From the slope of the plot $\Delta\eta$ - Y from Fig. 9 a value of the equivalent specific resistance of 10^8 ohm cm is estimated. The higher overpotential (or higher resistance of the process of the Li deposition in $LiClO_4$ can be attributed to the difficulty of the Li^+ transport from the solution/film to the film/metal interfaces. This effect, however, was not observed in $PC/LiAsF_6$ solutions where completely symmetric transients in both directions were recorded up to 10-15 mA/cm^2 (Fig. 10b).

A similar effect of asymmetric overpotential behavior of magnesium electrodes in $SOCl_2$ solutions was reported by Peled and Strase[18]. According to their assumption, the effect is due to the rather difficult process of solvated molecules shedding their solvent before entering the passivating layer. One should assume from the experimental results that the energy necessary for the shedding of molecules in Li deposition from $LiAsF_6$ solutions is lower than

from $LiClO_4$ solutions, because of the larger size of $LiAsF_6$. The effect is complicated by other factors such as the surface film sensitivity to the impurities, the influence of a secondary porous film, etc. The dependence of the excess cathodic voltage $\Delta\eta$ on film thickness (Fig. 9) is not consistent with solvent molecule shedding at the solution/passive layer interface.

6. Film Growth

As it was recently demonstrated[16] a good agreement with experimental results of the passive film growth in $SOCl_2$ - $LiAlCl_4$ solutions can be obtained if an additional slow film corrosion is taken into account. The corrosion rate is assumed to rule the growth of the secondary porous film in the postulated dual film model.

The same approach is used in this study especially for solutions containing 0.05% and 0.1% H_2O where the corrosion rate is higher.

The equations derived are:

$$v = (\partial Y/\partial t) = v_g - v_c \tag{13}$$

$$v = \frac{\Delta\phi V_m \kappa}{YF} - v_c \tag{14}$$

$$v = A/Y - v_c \; [cm/s] . \tag{15}$$

Here v is the instantaneous net rate of film growth calculated by graphical differentiation of the Y - t curves. v_g is the rate of the primary passive film growth by field assisted ionic migration in the solid phase, v_c is the rate of corrosion assumed to be independent of film thickness and time, $\Delta\phi$ is the potential difference in the film V_m is the molar volume of the passive film in cm^3/mole.

In Fig. 11 v is plotted vs. the reciprocal film thickness 1/Y. The slopes of the v-1/Y relations yield the kinetic constant A, the intercept with the abscissa gives the steady state thickness Y_∞ obtained when v = 0. Under this condition Eq. (15) yields the corrosion rate of the film:

$$v_c = \frac{A}{Y_\infty} \; [cm/s] . \tag{16}$$

Table III presents the kinetic data obtained from the plots in Fig. 11. For

comparison, data on Li in $SOCl_2$/$LiAlCl_4$ [16] are also included.

Film growth rates derived from simultaneous ellipsometric measurement in the same solutions [19] are of the same order of magnitude as those presented in Table III. For example, ellipsometry gives for v_c in PC/1M $LiClO_4$ solution with 0.1% H_2O a value of 0.15 - 0.3 x 10^{-12} cm/s, assuming a constant growth of the porous film during 10 days of storage.

As should be expected, corrosion rates of Li in PC solutions are two orders of magnitude lower than in $SOCl_2$-$LiAlCl_4$ solutions. This, on the other hand, explains the negligible voltage delay problems in Li/PC batteries as compared to Li/$SOCl_2$. However, according to the results presented, the voltage delay in PC electrolyte batteries is expected to increase at longer periods of battery storage and higher water contents (0.05-0.1%).

7. Surface Film Observations

(a) Scanning Electron Microscopy (SEM)

The SEM pictures of lithium stored in pure PC, waterfree solutions of $LiClO_4$ and $LiAsF_6$, as well as solutions of $LiClO_4$ and $LiAsF_6$ with 0.1 percent H_2O are presented in Figs. 13-18. Figure 12 presents the bare lithium surface before its immersion in PC solutions. The transfer time of all lithium specimens from the glove box to the SEM was approximately 1 hr. A special transfer device was built, in which the specimen was contained in a partial vacuum of 10-20 μ of helium. For easier comparison, most of the pictures are presented at 15,000 x magnification.

Figure 13 is taken from the Li stored for 40 days in pure PC; Figs. 14 and 15 from PC/0.5 M $LiClO_4$ solution after approximately 2-4 weeks; Fig. 16 from PC/0.5 $LiAsF_6$, and PC/1M $LiClO_4$, respectively, with 0.1 percent H_2O after 6-days of storage.

In parallel with electrochemical cells, Li specimens were stored in closed containers in the glove box in the same solution as in the cells. There

were no observable differences in the microstructure between samples stored in the glove box and those from electrochemical cells which were kept in air.

From the pictures presented, it is quite obvious that the film morphology depends on the electrolyte composition as well as on storage time. With higher water concentration and longer storage time, a coarser crystalline film with higher porosity was observed. At low water concentration, the morphology of the film formed in $LiClO_4$ (Figs. 14-15) is different from that in $LiAsF_6$ (Fig. 16). However, nearly the same rough and porous structure was observed in both solutions when the water level was increased to 0.1 percent (Figs. 17 and 18).

The fact that the Li corrosion in propylene carbonate containing 0.1 percent H_2O is decreased by the presence of electrolyte salt is demonstrated in Figs. 19-23. All specimens were taken from the solutions after five days of storage in the glove box.

Figure 19 is of Li in PC, containing 20 ppm H_2O at 15000 magnification.

Figure 20 - PC + 0.1 percent H_2O, 1000x

Figure 21 - PC + 0.1 percent H_2O + 0.2 m $LiClO_4$; 1000x

Figures 22 and 23 - is in PC + 0.1 percent H_2O + 1.2 m $LiClO_4$, respectively, at 2000 and 15000 magnifications.

The microstructure shown by the pictures supports the assumption given in sections 4 and 6 about the very important role of the electrolyte salts in propylene carbonate for film growth and lithium corrosion.

The increase in $LiClO_4$ (or $LiAsF_6$) concentration from 0.2 M (Fig. 21) to 1.2 M (Figs. 22 and 23) drastically decreases the lithium corrosion and reduces the influence of higher water concentration (0.1 percent) on lithium secondary film formation.

A comparison of Li surface layers formed in PC with 20 ppm H_2O (Fig. 19) with those formed with 1000 ppm and 1.2 M $LiClO_4$ (Fig. 23) also shows that at higher salt concentrations the effect of water on film formation rate is

comparatively low.

The pore-free, dense structure shown in Fig. 13 is consistent with electrochemical experiments mentioned before (see Sec. 1). Of course, it is difficult from the SEM examinations to conclude where nonporous film formation ends and porous films start. In this study, the porous film was assumed to possess low protective properties, and because of this, it influences the investigated Li passivity to a negligible extent. This assumption is probably not valid for longer storage times. Electrochemical measurements on nonporous primary films formed up to 5-6 days avoid the possible screening by a porous overlayer and were, therefore, considered to be more precise.

(b) Auger Electron Spectroscopy (AES)

Auger spectra and depth profiles on Li electrodes stored in different PC solutions were taken. The most reproducible results were obtained from lithium stored in pure propylene carbonate (without salts).

An Auger spectrum of lithium stored for 2 weeks in the glove box is shown in Fig. 24, its 5 min. depth profile (in atomic percentages) is given in Fig. 25, and a spectrum of a fresh Li surface is shown in Fig. 26.

The main detected elements and their Auger energies are as follows: Li - 47 eV, 0 - 510 eV, C -267 eV.

The sputtering rate for the present films under the experimental conditions of 3 keV - 15 nA of argon ion beam is unknown; however, the corresponding sputtering rate on Ta_2O_5 is 150 Å/min.

If the bare Li surface is assumed to be reached after 3-4 min of sputtering with the Ar ion beam (Fig. 25), a film thickness of approximately 400-500 Å is derived on the basis of the Ta_2O_5 sputter rate. This value is very close to that determined by the electrochemical measurement of the electrode capacitance under similar conditions (8-10 days in pure PC) and was found to be 300-350 Å (0.12-0.14 $\mu F/cm^2$ at ϵ = 5). In Table IV,

the lithium surface composition calculated from the presputtering AES analysis is compared to stoichiometric ratios of lithium compounds reported to be formed on a Li-surface from this solution [1, 11, 12, 13] (different ratios may be obtained from calibration runs). The table illustrates the atomic ratio between oxygen, carbon, and Li in Li_2O, LiOH, and Li_2CO_3 compared to that derived from AES analysis of the surface film.

From Table IV, one can see that both Li_2CO_3 and LiOH may exist in the surface layer. However, the surface analysis taken from the bare Li surface before its contact with the electrolyte has also shown the same carbon content (Fig. 22). The source of carbon may be contamination in the UHV chamber caused by previous users. This makes the calculations of the carbon ratio uncertain as well as the final conclusions of the film composition.

The pre-sputter atomic ratios did not differ for surface layers formed in $LiClO_4$ or $LiAsF_6$ solutions. However, there was a change in the depth profile scans, especially from the electrodes stored for longer times, due to some inhomogeneity of the porous film.

An organic polymer nature of surface layers in propylene carbonate solutions, has been reported recently.[13] SIMS analysis on the same specimen used for AES were also made in this study. From SIMS spectra, there was no evidence for PC polymerization products.

8. Underline General Discussion and Conclusions

All presented results support the notion that the passivity of Li in PC solutions at open-circuit and ambient temperature can be attributed to the formation of a thin nonporous and electronically insulating film.

The origin of this passive layer remains not completely clear. The increase of film formation rate at higher water concentration and the independence of the specific conductivity of the films of the water level in $PC-LiAsF_6$

solutions support the assumption that the reaction of Li with water is favored in propylene carbonate solutions. This is also supported by the presented SEM and AES observations. As was already mentioned, this is consistent with results of Butler et al.[12] Besenhard and Eichinger[20] have pointed out that 4×10^{-2} ppm H_2O are sufficient to form a monolayer of LiOH on a smooth Li surface of 1 cm^2 exposed to 1 cm^3 electrolyte. This example related to the experimental conditions of this study (50 cm^3 electrolyte, 5 cm^2 electrode and 20-50 ppm H_2O) leaves no doubt about the existence of this probability.

Recently, David et al.[17] and Keil et al.[21] have shown that even at extremely low oxygen exposures (66 Langmuirs) the freshly cut Li surface is immediately covered by Li_2O film. Under practical conditions of our He flushed dry box (2-5 ppm H_2O and O_2) the exposure dose is much higher and one should always take into account a thin oxide film on the Li surface.

The following reactions in PC solutions are possible (thermodynamic data are listed in Table V):

$$2 \ Li + \tfrac{1}{2} \ O_2 = LiO_2, \quad \Delta G° = -137.7 \ \text{kcal/mole} \qquad (a)$$

$$3 \ Li + \tfrac{1}{2} \ N_2 = Li_3N, \quad \Delta G° = -37.3 \ \text{kcal/mole} \qquad (b)$$

$$\tfrac{1}{2} \ Li_2O + \tfrac{1}{2} \ H_2O = LiOH, \quad \Delta G° = -8.9 \ \text{kcal/mole} \qquad (c)$$

$$Li + H_2O = LiOH + \tfrac{1}{2} \ H_2, \quad \Delta G° = -49.4 \ \text{kcal/mole} \qquad (d)$$

$$2 \ Li + H_2O = Li_2O + H_2, \quad \Delta G° = -81.0 \ \text{kcal/mole} \qquad (e)$$
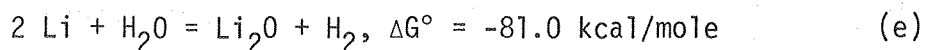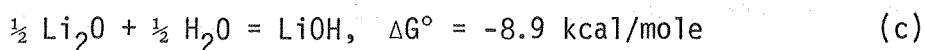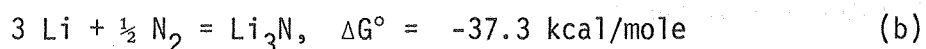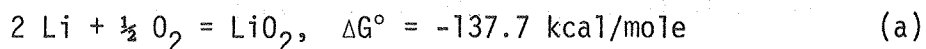
A slow reaction between Li and the solvent by means of Li^+ migration through the solid phase is not excluded to also occur:

$$2 \ Li + C_3H_6CO_3 = Li_2CO_3 + C_3H_6 \qquad (f)$$
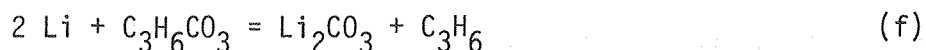
Brummer et al.[23] have shown that small amounts of water increase the stability of PC and THF due to the formation of solvent impermeable films. This observation supports the above-proposed mechanism.

The same authors have found that AsF_6^- improves the Li cycling efficiency in PC solution, probably as a result of the higher conductivity of the film formed in AsF_6^- containing solutions as compared to films from ClO_4^- solutions.

As shown in this study, the conductivity of the passive film formed in PC/LiAsF$_6$ is 2-3 times higher than that in PC/LiClO$_4$. The voltage in excess of the process of the Li deposition in LiClO$_4$ solutions probably also worsens the cycling Li efficiency as compared to that in PC/LiAsF$_6$.

With a dielectric constant of 5, assuming that ε does not depend on the solute and the film density, a field constant B, typical for barrier films, was derived. This value for PC/LiAsF$_6$ is $1.8 \pm 0.2 \times 10^{-6}$ V^{-1} cm, and for PC/LiClO$_4$ solutions is 0.8 to 1.3×10^{-6} V^{-1} cm, dependent on the water content. This agreement of the experimental results with the basic equation of the ionic transport, and especially the accuracy of the experimentally found thickness used for calculating the kinetic constants, could be determined once more.

Following Young,[10] the Eq. (2) $i = i_0 \exp(BE)$ is valid when the backward current is negligible compared to the forward current. Hence, the ratio P will indicate this validity:

$$P = \exp-(W - qaE)/\exp-(W + qaE) \qquad (15)$$

where W is the activation (barrier) energy, q is the ion charge of the mobile ion, a is the half-jump distance, and E is the field strength.

The apparent activation energy of the ionic conductivity was assessed by the temperature dependence of κ of the passive film, formed in PC/0.5 m LiClO$_4$ in the temperature range -20 to +20°C. The Arrhenius plot (Fig. 22) yields 0.61 V. This value with a = 3Å and q = 1e for a field E = 10^6V/cm gives P $\simeq$ 10. This means that at electric fields of 10^6V/cm a Tafel-like behavior is expected. The experimental results summarized in Figs. 4 and 8 have confirmed this theoretical expectation.

If instead of the thicknesses of the nonporous film, measured by the pulse galvanostatic technique, the values of the thickness derived from ellipsometry[19] had been used for the field strength determinations, disagreement with Eq. (2) would have been obtained.

As it was shown, the passive film formed in PC solutions is an electronic insulator with conductivity 2 to 5 x 10^{-9} ohm^{-1} cm^{-1}. It is difficult for electronic insulators like LiOH or Li_2CO_3 to explain the film growth at electric fields as low as several hundred volts per cm. Attempts for explanation of this phenomenonon for LiCl films in $SOCl_2$ solutions have been made.[16]

Recently, a theoretical model for dual-film growth on Li in $SOCl_2$ solutions has also been proposed by Hermann.[22]

As was shown in Sec. 6, a similar dual-film model independent from that proposed by Hermann proved to explain satisfactorily the experimental results obtained for passive films growing in propylene carbonate solutions. A corrosion rate of (1 to 4)x10^{-12} cm/s derived from Eq. (13) agrees with the film growth rate of porous films measured simultaneously by ellipsometry.

During this study a few points have also remained unclear that could be summarized in the following questions deserving further efforts for elucidation:

1. What is the role of the solute, especially $LiClO_4$ and $LiAsF_6$, in the passive film formation mechanism.

2. Why does the same water content of 0.1 percent which results in similar film microstructure cause a decreased film conductivity for $LiClO_4$/PC solutions while film conductivity is not affected for PC/$LiAsF_6$.

3. Why does Li electrodeposition from PC/$LiAsF_6$ solutions occur without an excess overvoltage as compared to PC/$LiClO_4$ solutions, where overvoltage at longer storage times is significant.

4. What is the film composition and its dielectric constant.

5. Why does lithium corrode faster in propylene carbonate with 0.1 percent H_2O as compared to PC with the same H_2O concentration but containing 0.5-1.2 M $LiClO_4$ or $LiAsF_6$.

References

1. A. N. Dey, Thin Solid Films 43, 131 (1977).

2. E. Peled and H. Yamin, 18th Power Sources Symposium, 237 (1978).

3. E. Peled, J. Electrochem. Soc. 126, 2047 (1979).

4. R. V. Moshtev, Y. Geronov, B. Puresheva, and A. Nasalevska, 28th ISE Meeting, Varna, Extend. Abstr. 153 (1977).

5. A. Leef, A. Gilmour, J. Appl. Electrochem. 9, 663 (1979).

6. R. D. Rauh and S. B. Brummer, Electrochim. Acta 22, 75 (1977)

7. M. Garreau, J. Thevenin, and D. Warin, Progress in Batteries, Vol. 2, JEC Press, Cleveland OH, 1979, p. 54.

8. I. Epelboin, M. Froment, M. Garreau, J. Thevenin, and D. Warin, in Power sources for biomedical implantable applications and ambient temperature lithium batteries, B. B. Owens and N. Margalit, Eds., Vol. 80-4, Electrochemical Society, 1980, p. 417.

9. R. F. Scarr, J. Electrochem. Soc. 117, 295 (1970).

10. L. Young, Anodic Oxide Films, Academic Press, New York, 1961.

11. F. P. Dousek, J. Jausta, and L. Riha, J. Electroanal. Chem. 46, 281 (1973).

12. J. N. Butler, D. R. Cogley, and J. C. Synott, J. Phys. Chem. 73, 4026 (1969).

13. I. Epelboin, M. Froment, M. Garreau, L. Thevenin, and D. Warin, J. Electrochem. Soc. 127, 2100 (1980).

14. American Institute of Physics Handbook, McGraw-Hill, 1963.

15. Landolt-Börnstein, Vol. II, Part 6, p. 454, Springer 1959.

16. R. V. Moshtev, Y. Geronov, and B. Puresheva, J. Electrochem. Soc., in press.

17. M. H. Froning, T. N. Wittberg, W. E. Modeman, Abstr. 14, Electrochem. Soc. Meeting, Los Angeles, October 1979.

18. E. Peled and H. Straze, J. Electrochem. Soc., 1030, 124 (1977).

19. F. Schwager, Y. Geronov, R. Muller, Abstr. 3, Electrochem. Soc. Meeting, Hollywood FL, October 1980.

20. J. O. Besenhard and G. Eichinger, J. Electroanal. Chem. <u>68</u>, 1-18 (1976).

21. R. Keil, J. Hoenigman, W. Modeman, T. Wittberg, J. Peters, Interim Techn. Report, October 1979. AFWAL-TR-80-2018, Univ. of Dayton Research Inst., Dayton OH.

22. A. M. Hermann, Abstr. 61, Electrochem. Soc. Meeting, Hollywood FL, October 1980.

23. Circular 500, National Bureau of Standards, "Selected Values of Chemical Thermodynamic Properties" (1952).

24. Gmelin, vol. Li, Verlag Chemie, 1960.

TABLE I

Dielectric Constants of Electrolyte and Potential Film Materials

Propylene Carbonate	65
Li_2CO_3	4.9
Li OH	--
Li_2O	7.9
Polyethylene	2.3

TABLE II

Comparison between Experimental and Theoretical Tafel Slopes

Y	b_{exp}	$b_{theor.} = 20Y$
Å	mV	mV
25	460	500
37	670	740
65	1150	1300
103	1840	2060
130	2400	2600
138	2650	2760
162	3155	3240

TABLE III

Kinetic Data of Film Growth in Different Media

ELECTROLYTE	Y_∞	$\kappa \times 10^9$	A	v_c
	Å	$ohm^{-1} cm^{-1}$	cm^2/s	cm/s
PC/0.5M $LiClO_4$, 0.1% H_2O	114	0.81	1.3×10^{-18}	1.15×10^{-12}
PC/1.0M $LiClO_4$, 0.1% H_2O	167	1.34	1.8×10^{-18}	1.08×10^{-12}
PC/0.5M $LiAsF_6$, 0.1% H_2O	167	5.3	4×10^{-18}	2.4×10^{-12}
$SOCl_2$/1M $LiAlCl_4$	200	0.64	2×10^{-16}	1×10^{-10}

TABLE IV

Atomic Ratios Expected for Different Film Materials and Results
Obtained for Surface Layers by Auger Spectroscopy.

Compounds	Atomic Ratio		
	O/Li	C/Li	O/C
Li_2CO_3	1.5	0.5	3.0
Li_2O	0.5	-	-
LiOH	1.0	-	-
Surface layer			
a) presputter	1.25	1.2	1.15
b) 1-min. sputter time	1.15	0.30	4.0

TABLE V

Standard Enthalpies and Free Energies of Formation
from the Elements at 25°C, kcal/mole

Compound	State	ΔH°_{298}	ΔG°_{298}	Reference
Li_2O	c	-142.4	-137.7	23;24
Li_2O_2	c	-151.7	-135	23;24
Li_3N	c	- 47.17	- 37.33	23;24
$LiCl$	c	- 97.7	- 92.16*	23;24
$LiOH$	c	-116.45	-106.1	23
Li_2CO_3	c	-290.54	-270.66	23
H_2O	l	- 68.32	- 56.69	23

*calculated from entropies Ref. 24.

Figure Captions

Fig. 1 - Typical potential-time transients on a Li electrode in propylene
         carbonate solutions. (a) Short current pulses for capacitance
         measurements. 2, 4 - 0.1 mA/cm^2; 1, 3 - 0.2 mA/cm^2; scales 1:V=5mV/div,
         t=2μs/div; 2: V=2mV/div, t=2μs/div; 3: V=5mV/div, t=1μs/div; 4: V=2mV/div,
         t=1μs/div. (XBB 800-14741-A). (b) Long current pulses for overpotential
         measurements. 1 - 1 mA/cm^2, 2 - 2 mA/cm^2, 3 - 4 mA/cm^2, 4 - 8 mA/cm^2,
         5 - 10 mA/cm^2, 6 - 11.5 mA/cm^2, 7 - 13.3 mA/cm^2, 8 - 14.9 mA/cm^2;
         scale V = 0.5 V/div, t = 1 ms/div. (XBB 800-14739-A).

Fig. 2 - Tafel plots at constant film thickness (derived for ε = 5, anodic
         polarization), 1 - 25 Å, 7 - 37 Å, 3 - 65 Å, 4 - 103 Å, 5 - 130 Å,
         6 - 138 Å, 7 - 162 Å. (XBL 806-10429).

Fig. 3 - Relationship between film thickness Y and Tafel slope b. (XBL 8012-
         13349).

Fig. 4 - Tafel plots, log i vs. E, in different propylene carbonate solutions,
         30 - 200 Å films: 1-0.5M LiAsF$_6$, 2-0.5M LiClO$_4$, 3-0.5M LiClO$_4$ + 0.1% H$_2$O.
         (XBL 809-5972).

Fig. 5 - Reciprocal capacitance, 1/C vs. polarization resistance, R$_p$, in the
         following propylene carbonate solutions: o,● - 1M LiClO$_4$, ∇ - 1M
         LiClO$_4$ + 0.05% H$_2$O, ▼ - 1M LiClO$_4$ + 0.1% H$_2$O, □ - 0.5M LiClO$_4$ + 0.1% H$_2$O.
         (XBL 8012-13355).

Fig. 6 - Reciprocal capacitance, 1/C vs. polarization resistance R$_p$, in hexa-
         fluoroarsenate solutions. ●,o - 0.5M LiAsF$_6$, Δ - 0.5M LiAsF$_6$ +
         0.1% H$_2$O. (XBL 8012-13354).

Fig. 7 - Time - dependence of Li electrode resistance in different propylene
         carbonate solutions: 1-0.5M LiAsF$_6$; 2-0.5M LiAsF$_6$ + 0.1% H$_2$O; 3-0.5M
         LiClO$_4$; 4-0.5M LiClO$_4$ + 0.05% H$_2$O; 5-0.5M LiClO$_4$ + 0.1% H$_2$O.
         (XBL 8012-13352).

Fig. 8 - Tafel plots, log i vs. E, for: Δ - PC without salt, Y + 307 Å; $\square$ - PC/0.5M LiAsF$_6$, Y = 215 Å; o - PC/0.5M LiAsF$_6$ + 0.1% H$_2$O, Y = 205 Å. (XBL 8012-13350).

Fig. 9 - Dependence of the excess voltage, $\Delta\eta$, on the film thickness in 1M LiClO$_4$ at: 1-0.5 mA/cm^2, 2-1 mA/cm^2. (XBL 8012-13353).

Fig. 10 - Typical cathodic and anodic transients after 1 week in: (a) 1.0M LiClO$_4$, i = 0.5 mA/cm^2; upper trace (-) cathodic polarization, lower trace (+) anodic polarization: scales V = 20 mV/div, t + 2 ms/div. (XBB 800-13942-A). (b) 0.5M LiAsF$_6$, 1-0.5 mA/cm^2, 2-1 mA/cm^2; scales V = 20 mV/div, t = 2 ms/div. Cathodic and anodic transients are superimposed. (XBB 800-13943-A).

Fig. 11 - Dependence of the net rate of film growth, v, on the reciprocal film thickness, 1/Y. Propylene carbonate solutions with 0.1% H$_2$O: 1-0.5M LiClO$_4$, 2-1.0M LiClO$_4$, 3-0.5M LiAsF$_6$. (XBL 8012-13351).

Fig. 12 - SEM picture of bare Li surface, 15,000x. (XBB 800-11270).

Fig. 13 - SEM picture of Li in PC without salt, after 2 weeks of storage, 15,000x. (XBB 800-11281).

Fig. 14 - SEM picture of Li surface after 2 weeks of storage in 1M LiClO$_4$, 15,000x. (XBB 800-11274).

Fig. 15 - SEM picture of Li surface after 4 weeks of storage in 1M LiClO$_4$, 15,000x. (XBB 800-11287).

Fig. 16 - SEM picture of Li surface after 2 weeks of storage in 0.5M LiAsF$_6$, 15,000x. (XBB 800-11290).

Fig. 17 - SEM picture of Li surface after 1 week of storage in 1M LiAsF$_6$ + 0.1% H$_2$O, 15,000x.

Fig. 18 - SEM picture of Li surface after 1 week of storage in 0.5M LiClO$_4$ + 0.1% H$_2$O, 15,000x.

Fig. 19 - SEM picture of Li surface after 5 days of storage in PC containing 20 ppm H$_2$O, 15,000x (XBB 800-14896).
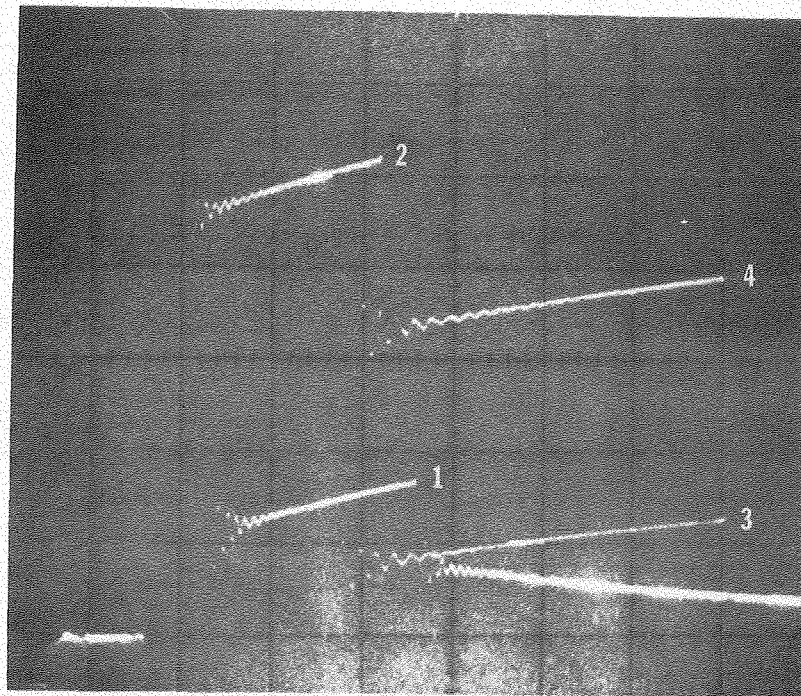
Figure 1a   XBB 800-14741-A
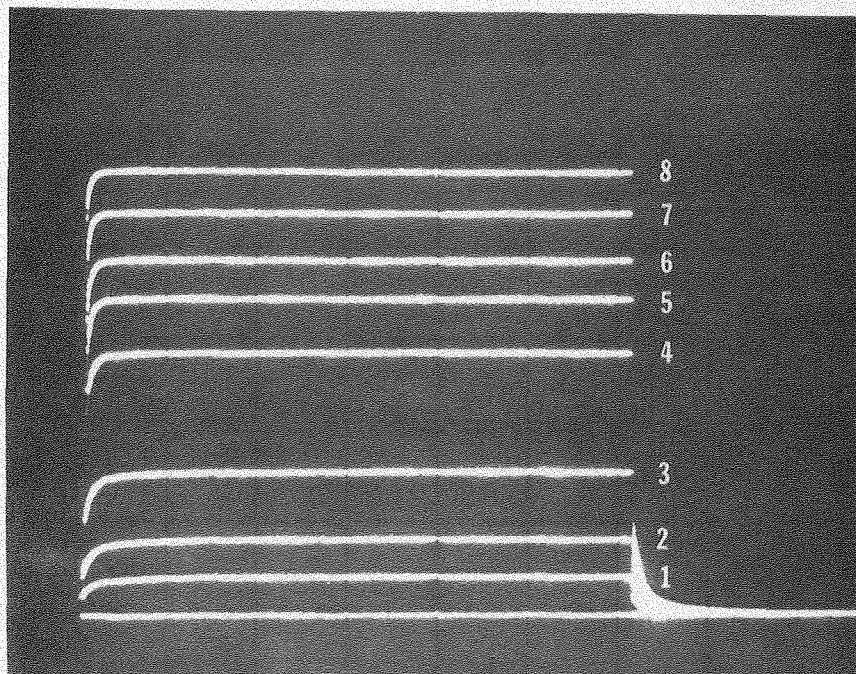
Figure 1b   XBB 800-14739-A
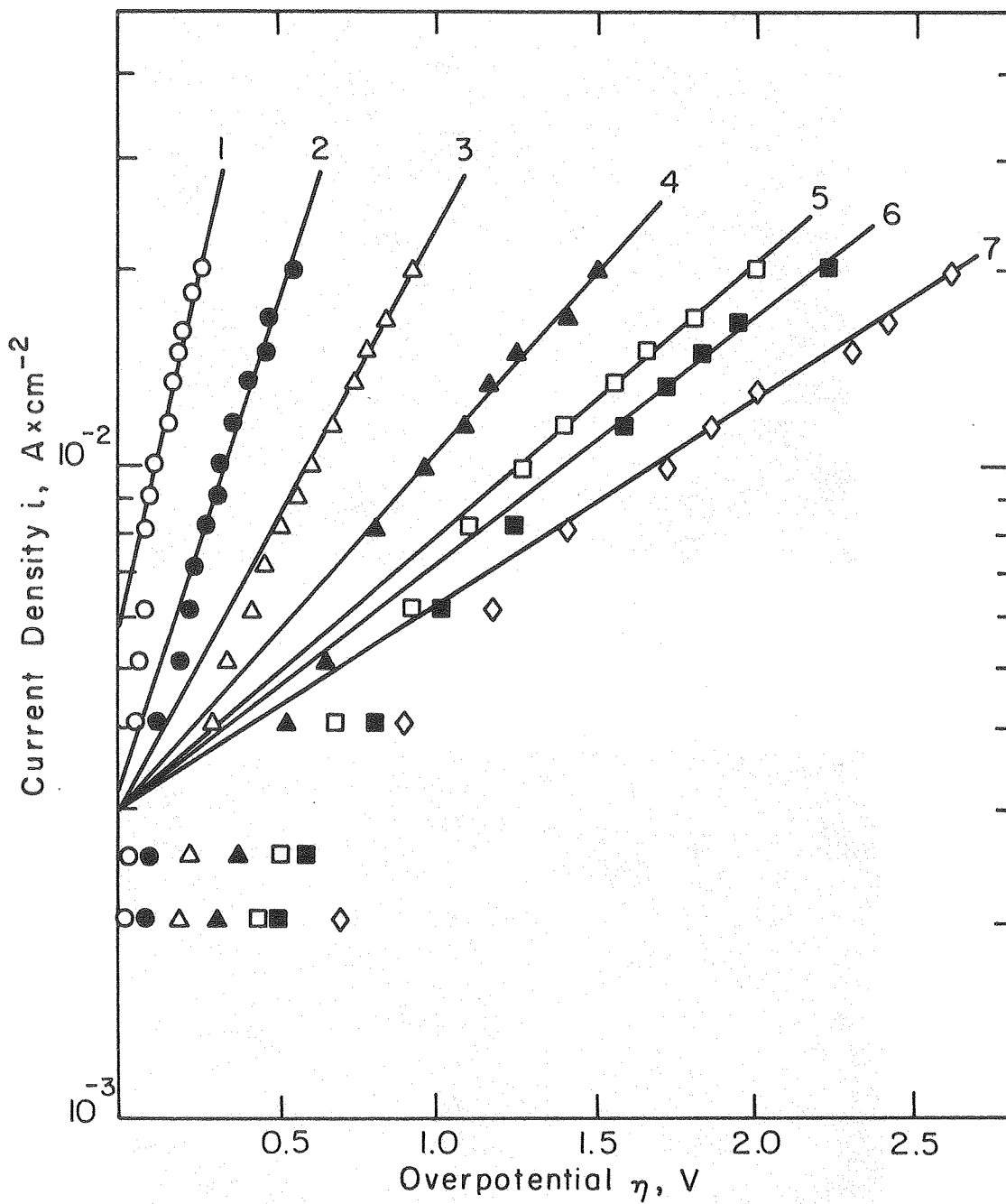
Figure 2

XBL 806-10429
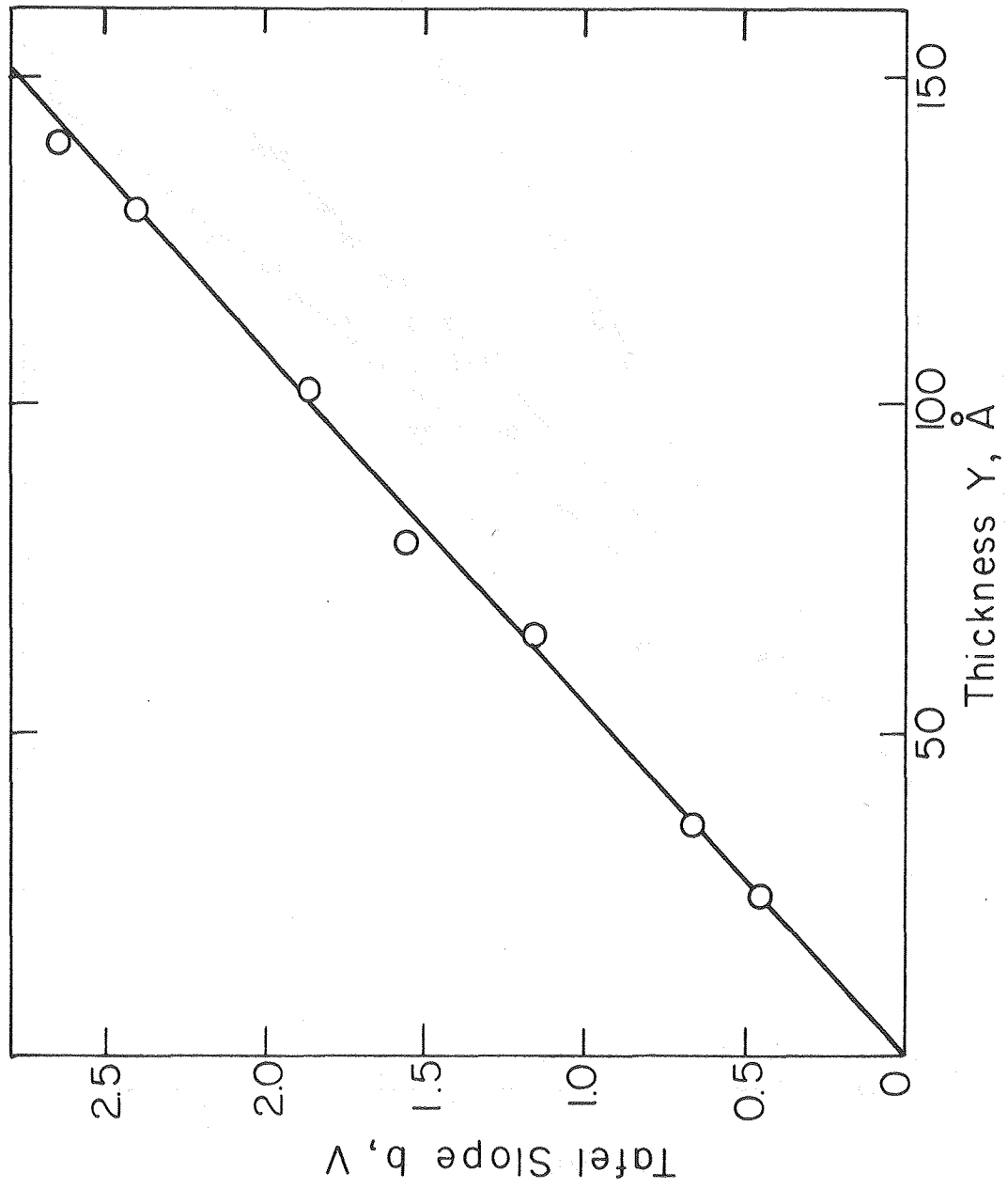
Figure 3

XBL 8012-13349
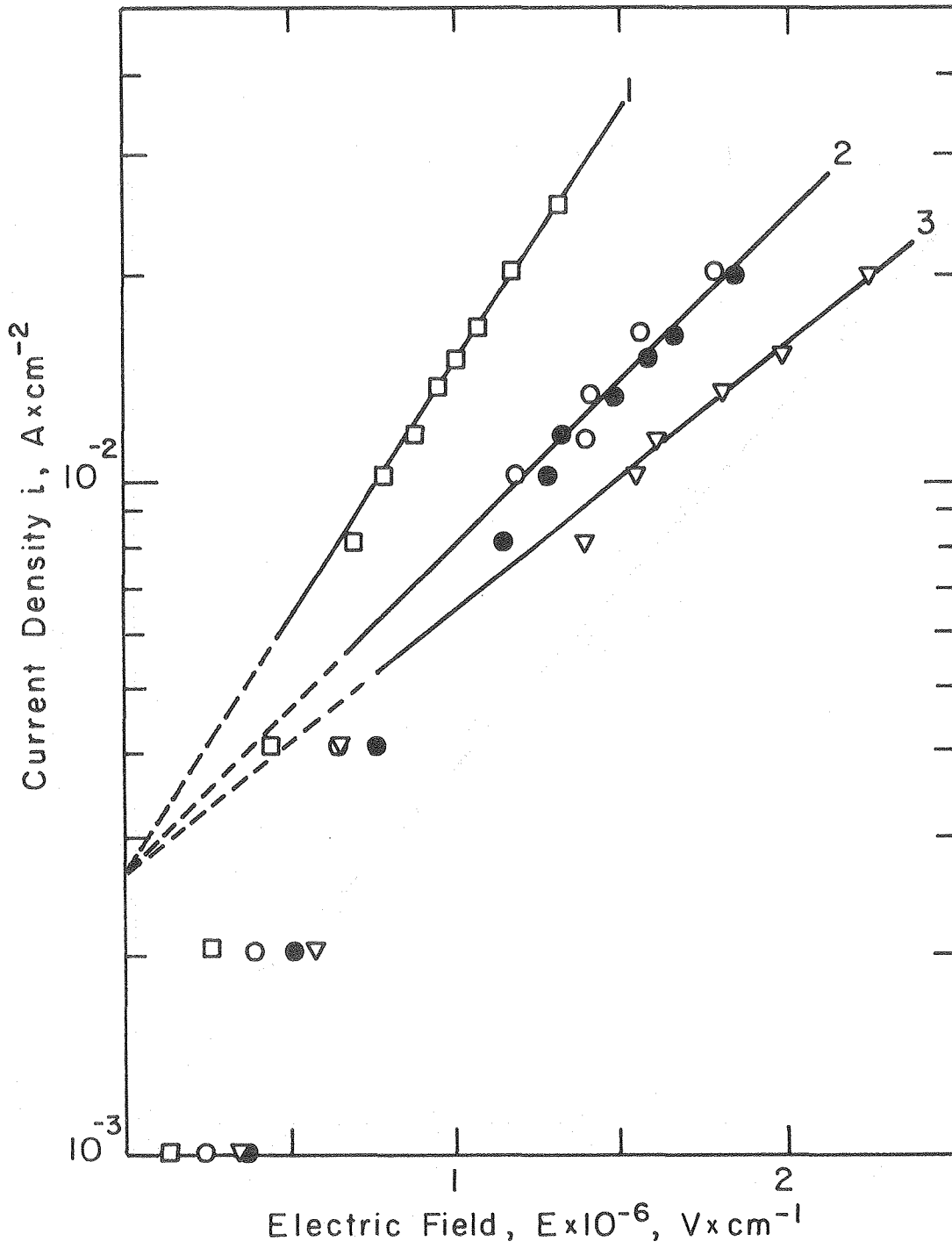
Figure 4

XBL 809-5972
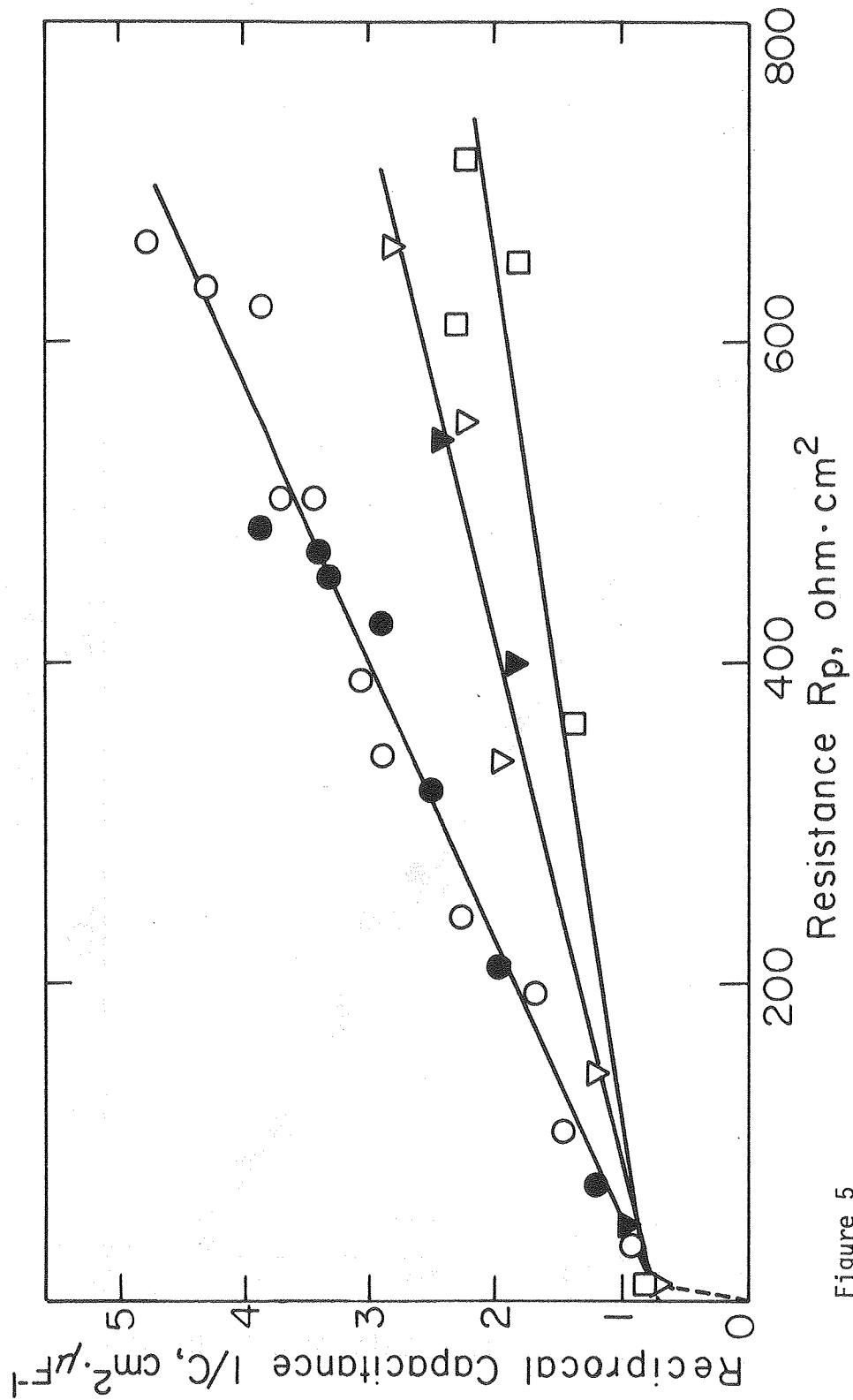
Figure 5
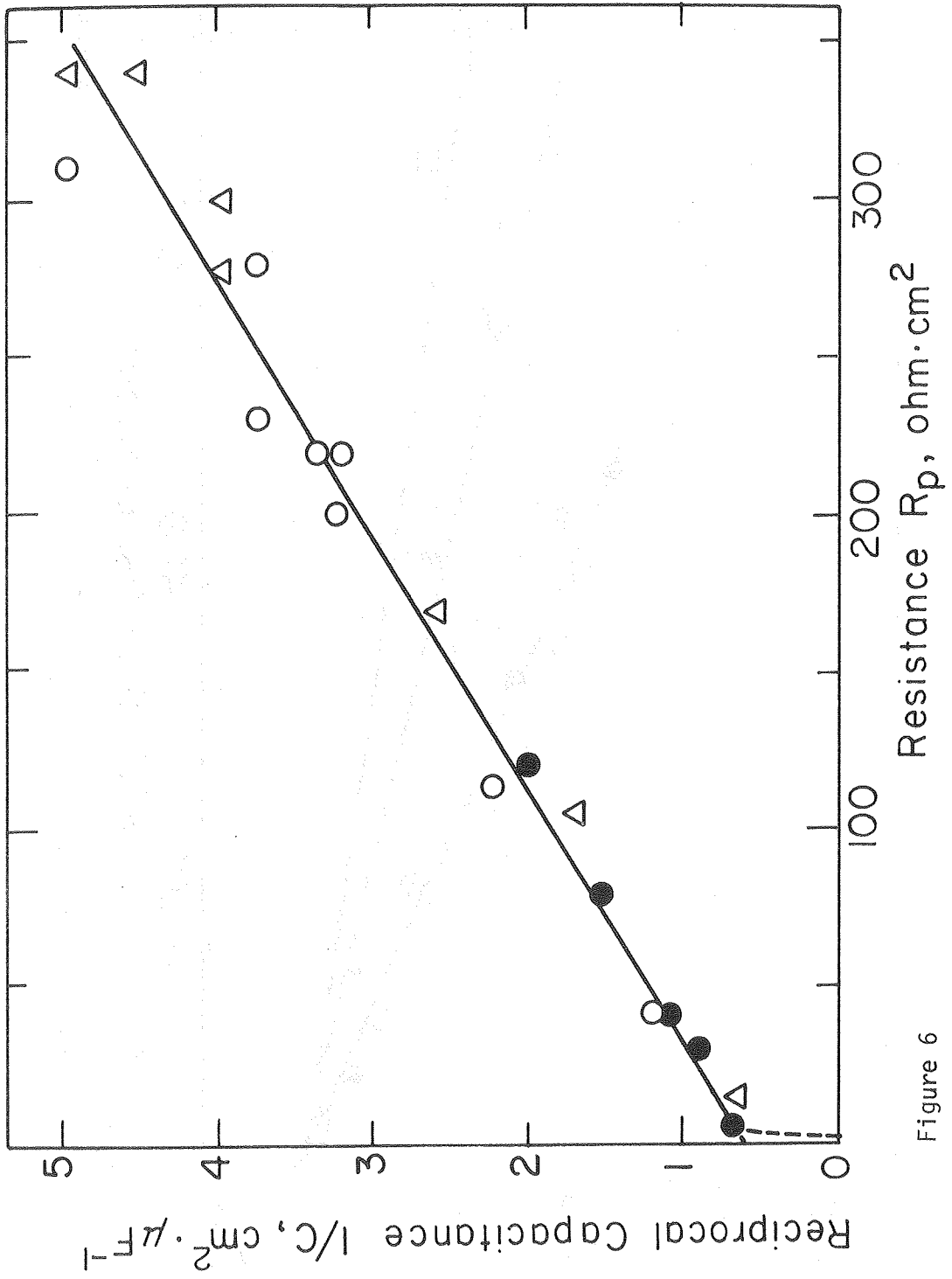
XBL8012-13355

Figure 6

XBL 8012-13354
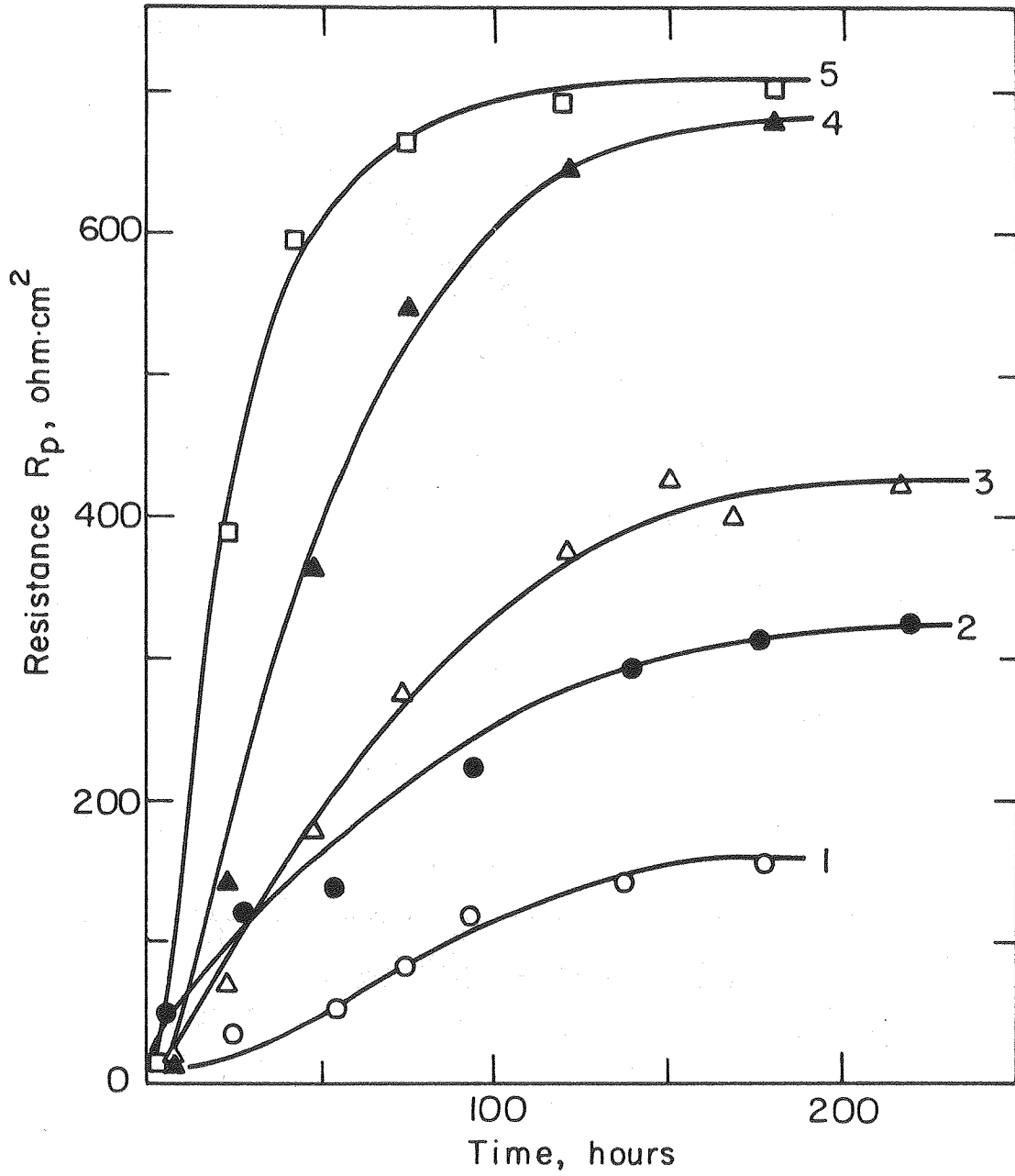
Figure 7

XBL 8012-13352
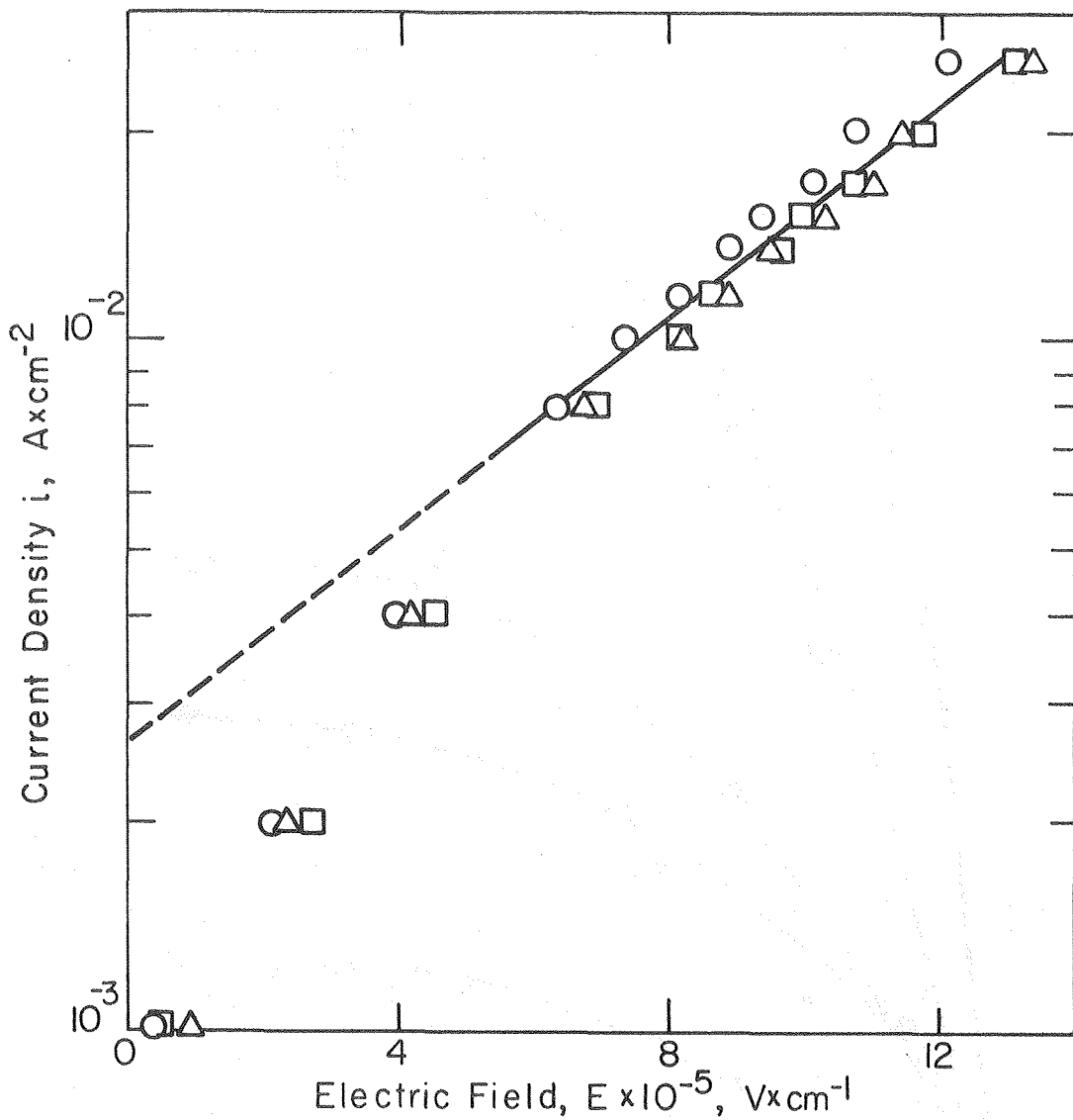
Figure 8

XBL8012-13350
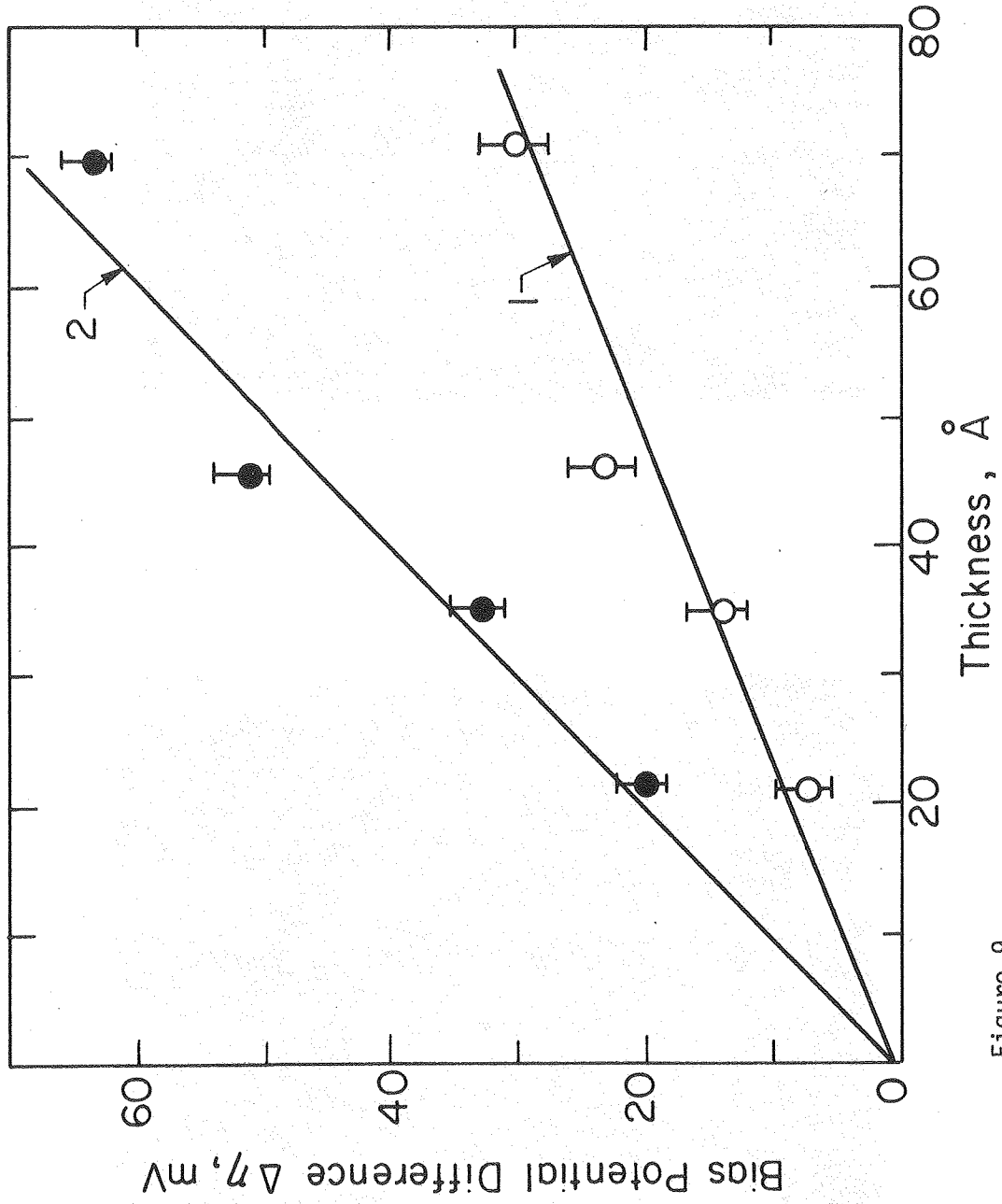
Figure 9

XBL8012-13353
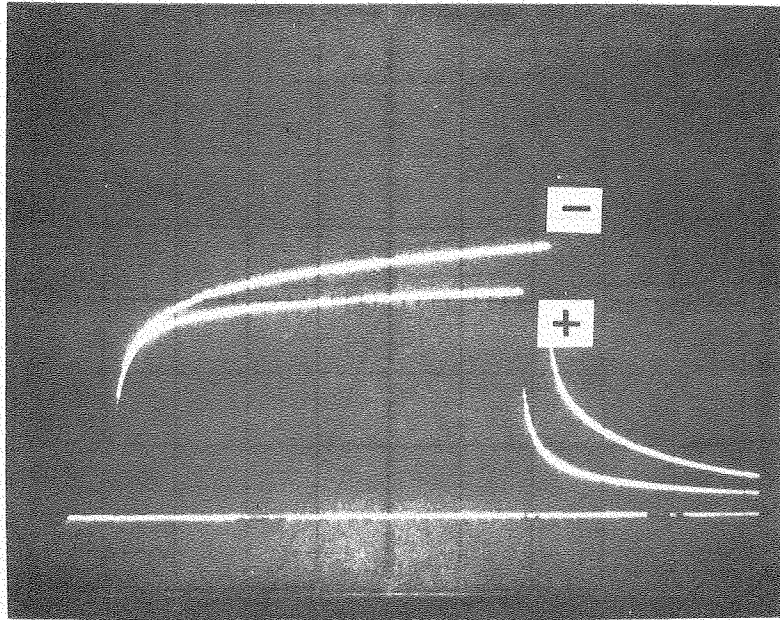
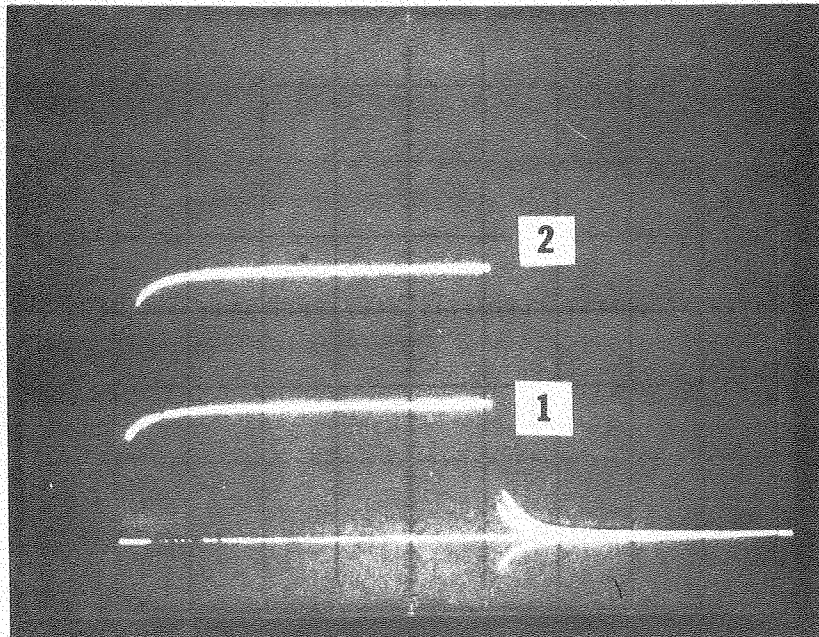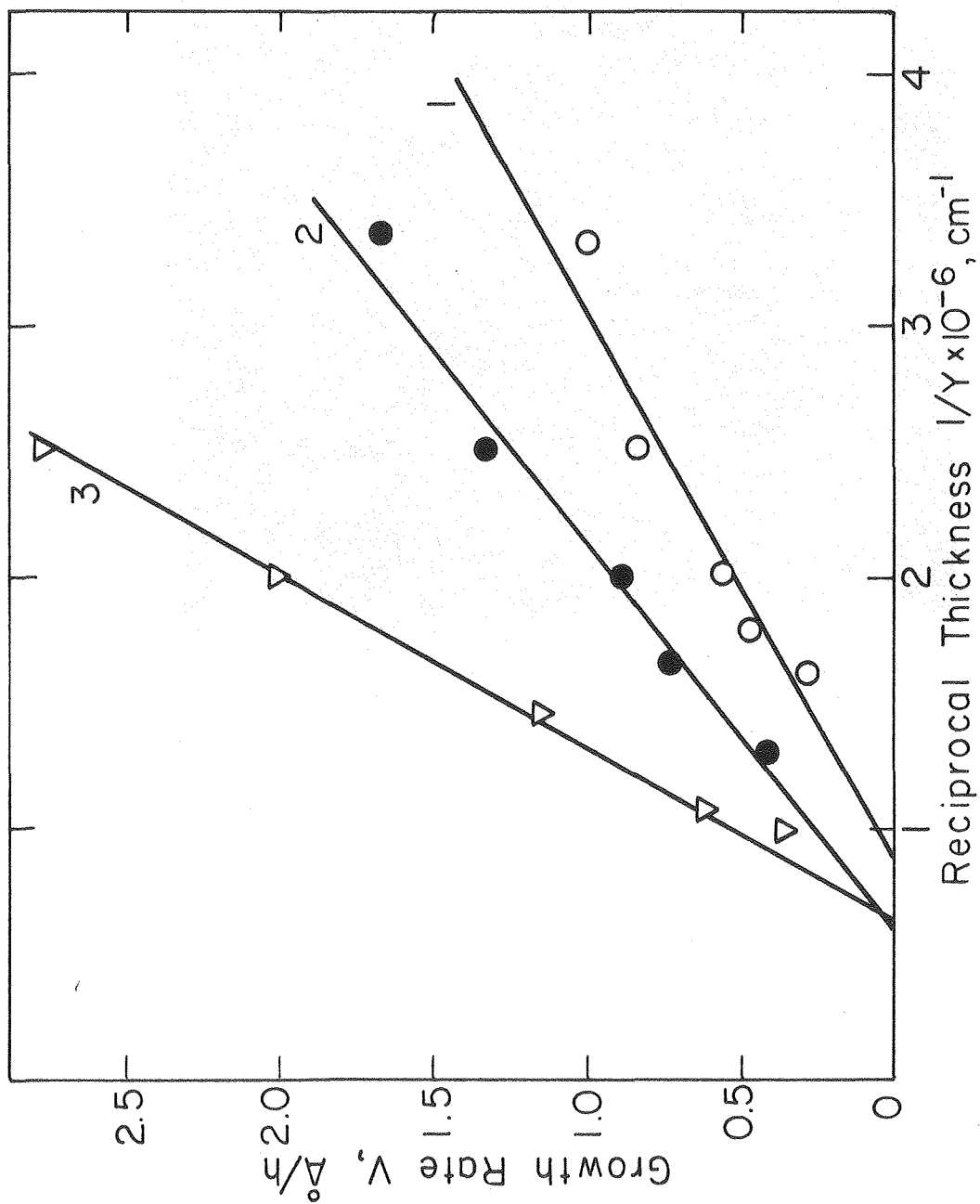Figure 10a   XBB 800-13942-A

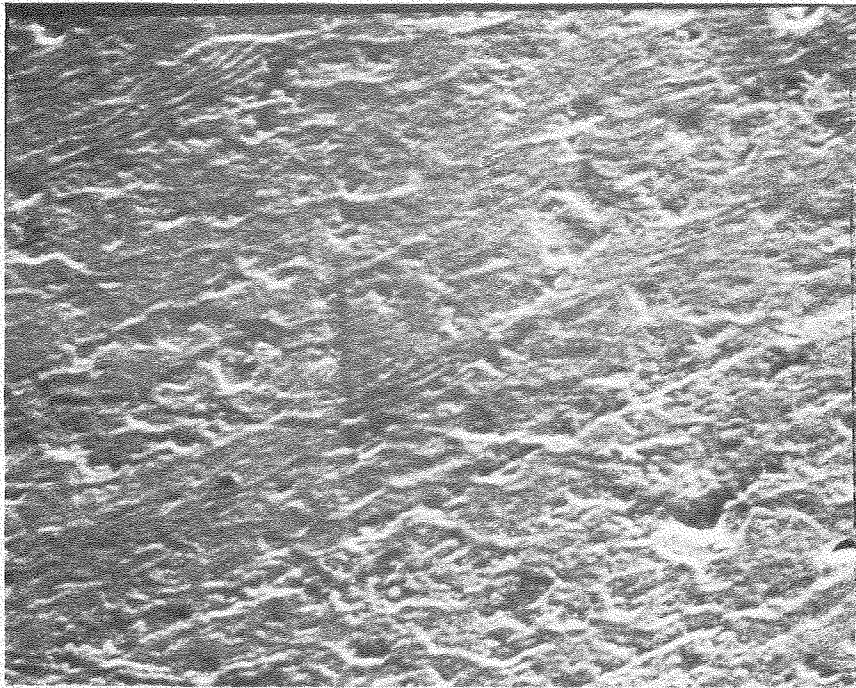Figure 10b   XBB 800-13943-A

Figure 11

XBL8012-13351

Figure 12   XBB 800-11270
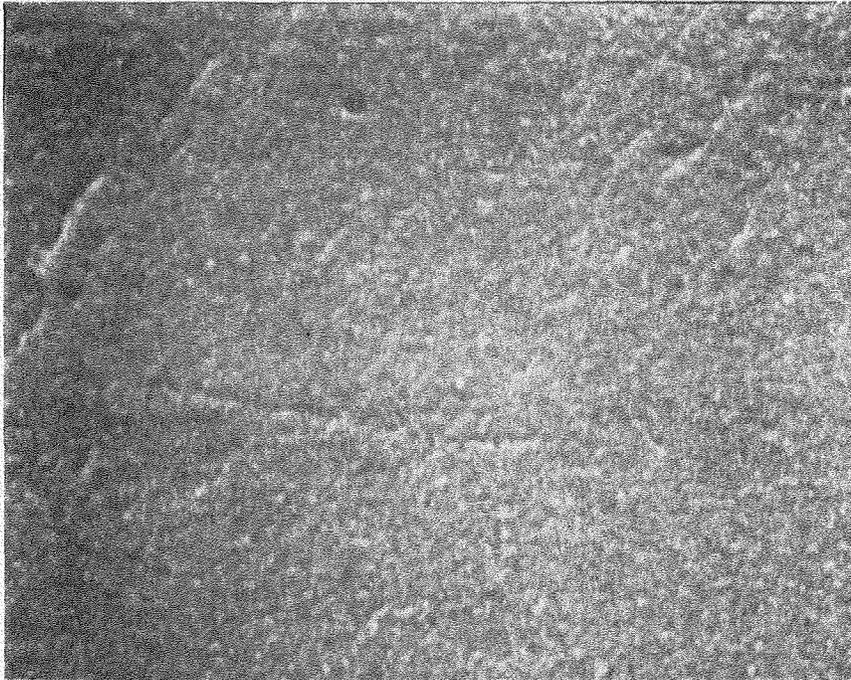
Figure 13
XBB 800-11281
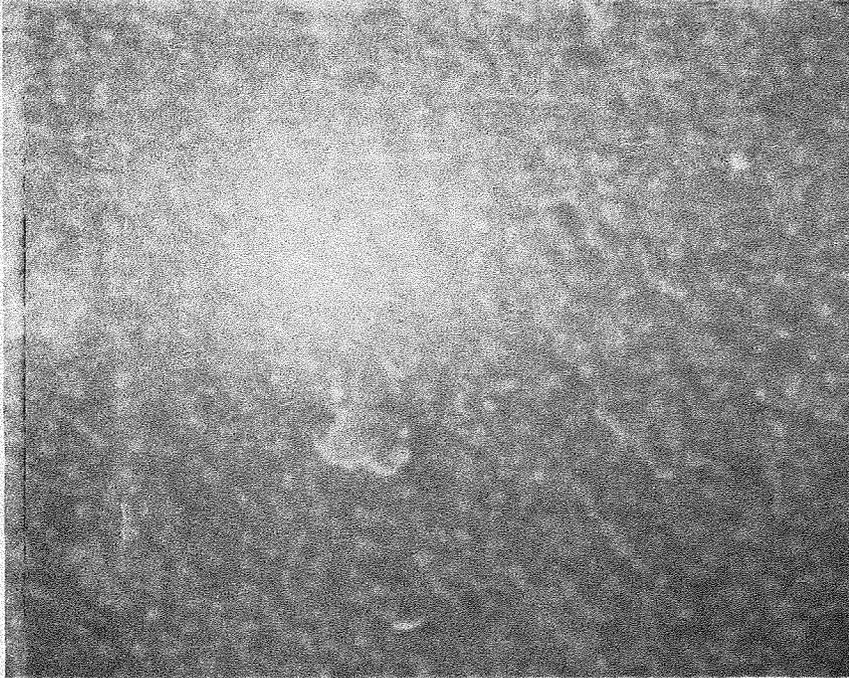
Figure 14   XBB 800-11274
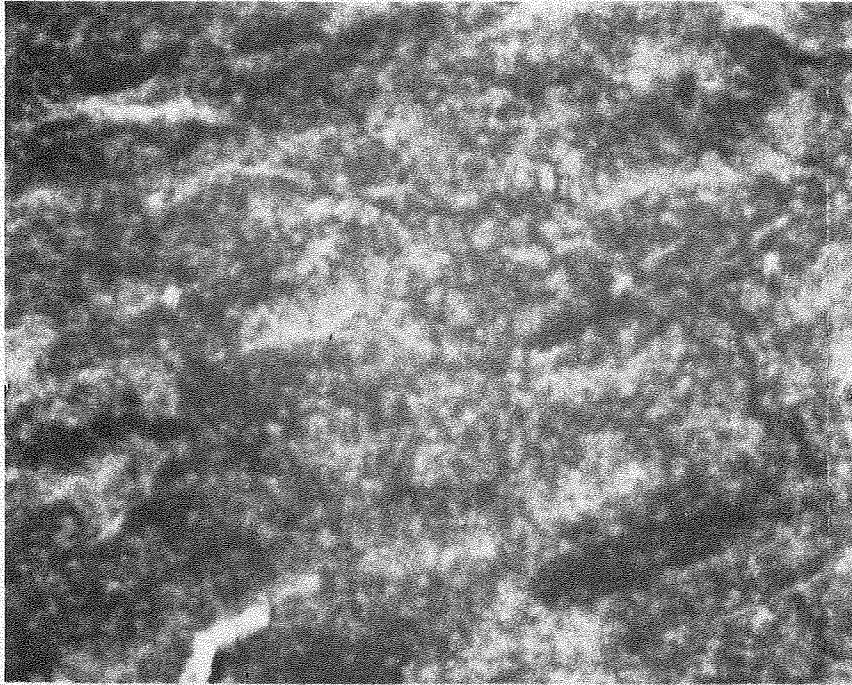
Figure 15   XBB 800-11287
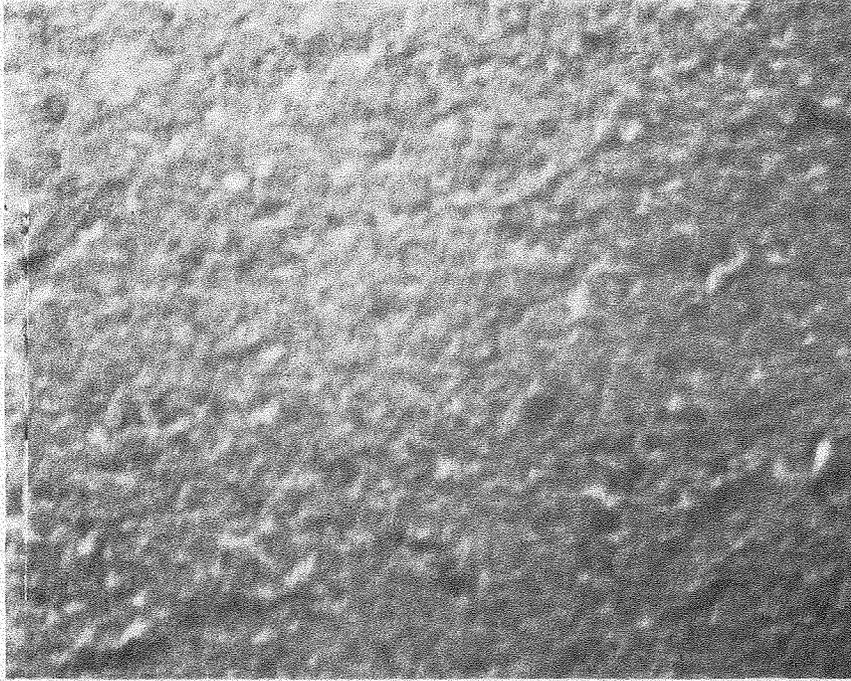
Figure 16   XBB 800-11290
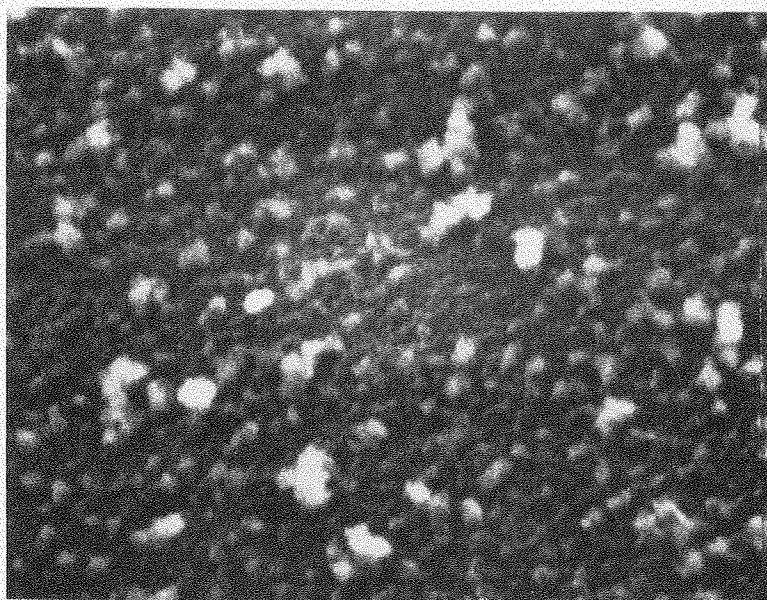
Figure 17   XBB 811-197
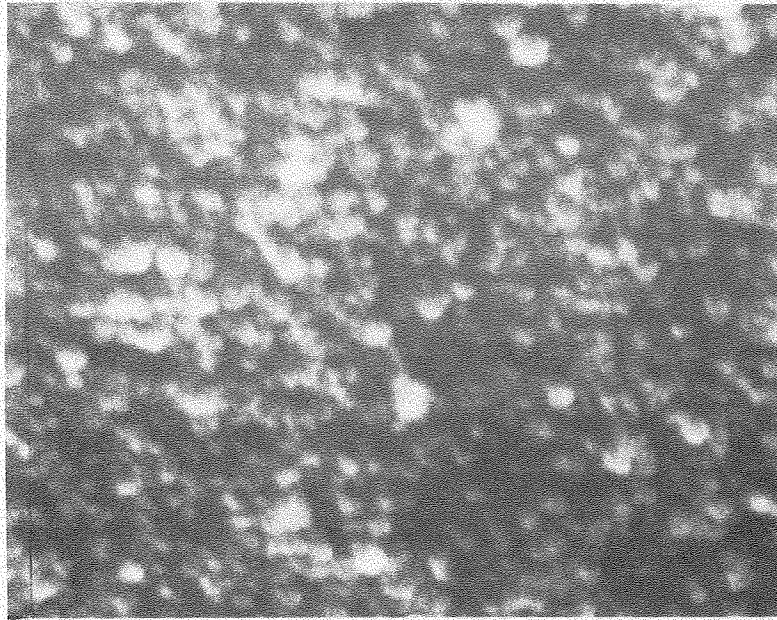
Figure 18   XBB 811-198
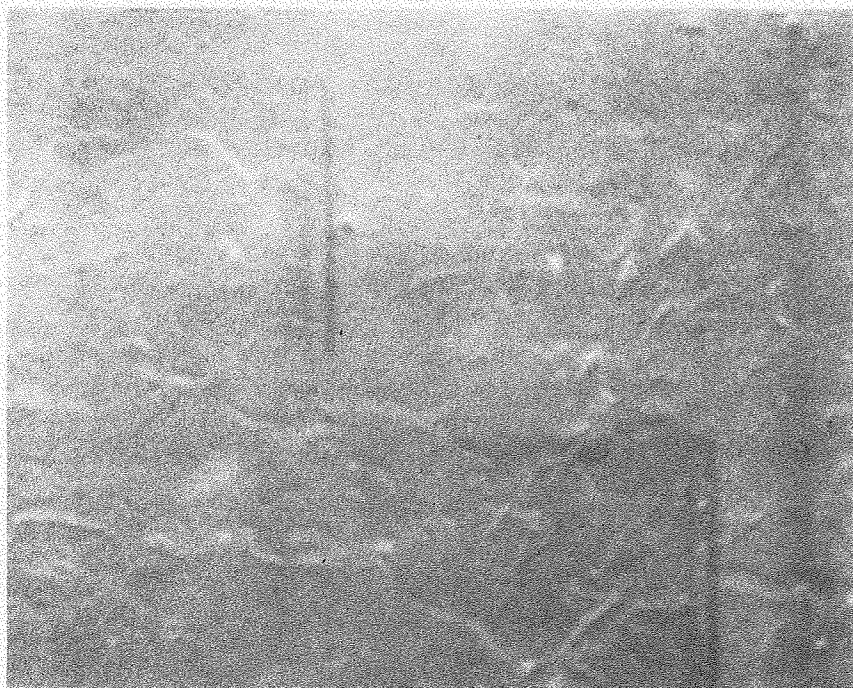
Figure 19   XBB 800-14896

Figure 20   XBB 800-14890
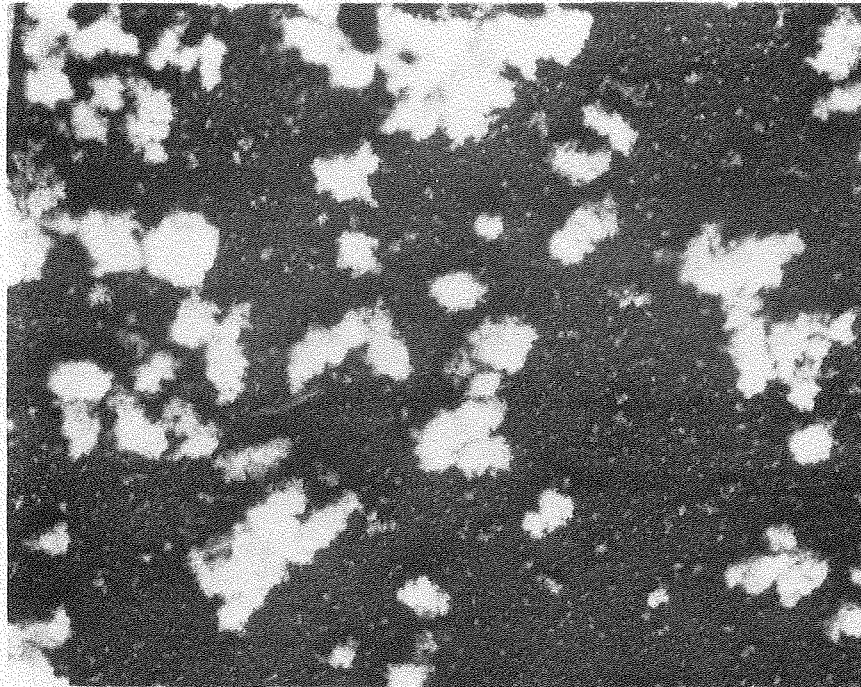
Figure 21   XBB 800-14895
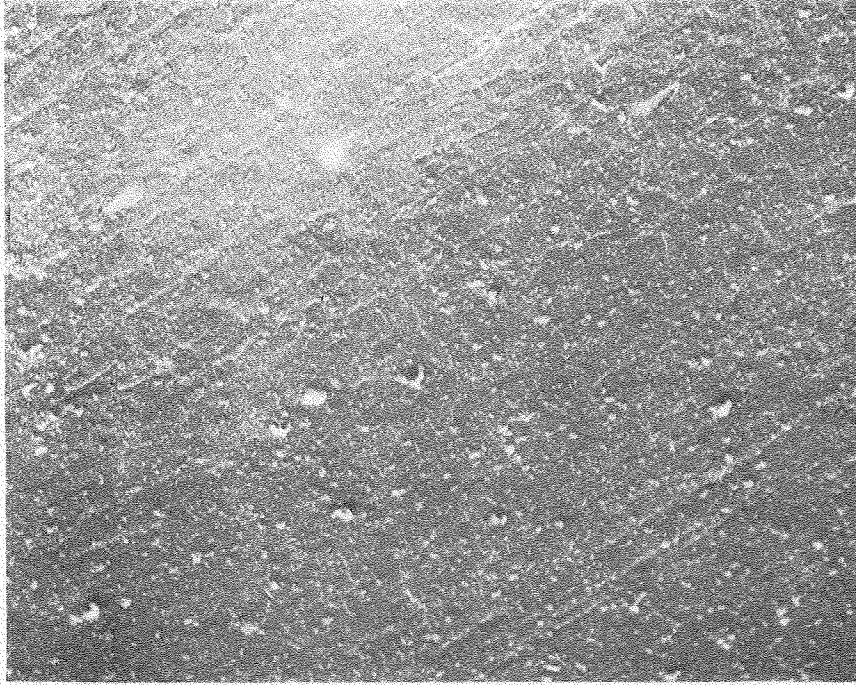
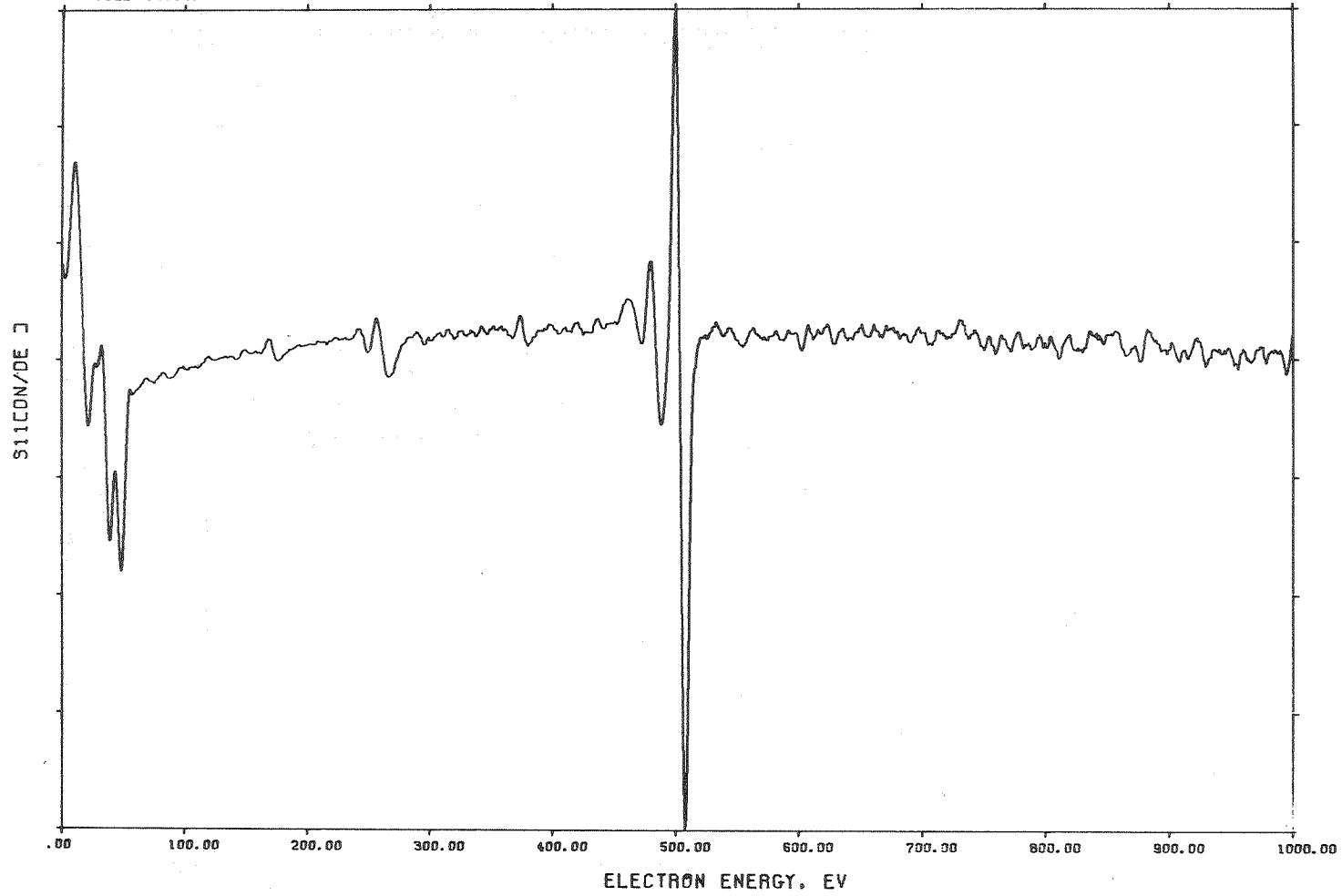Figure 22   XBB 800-14892
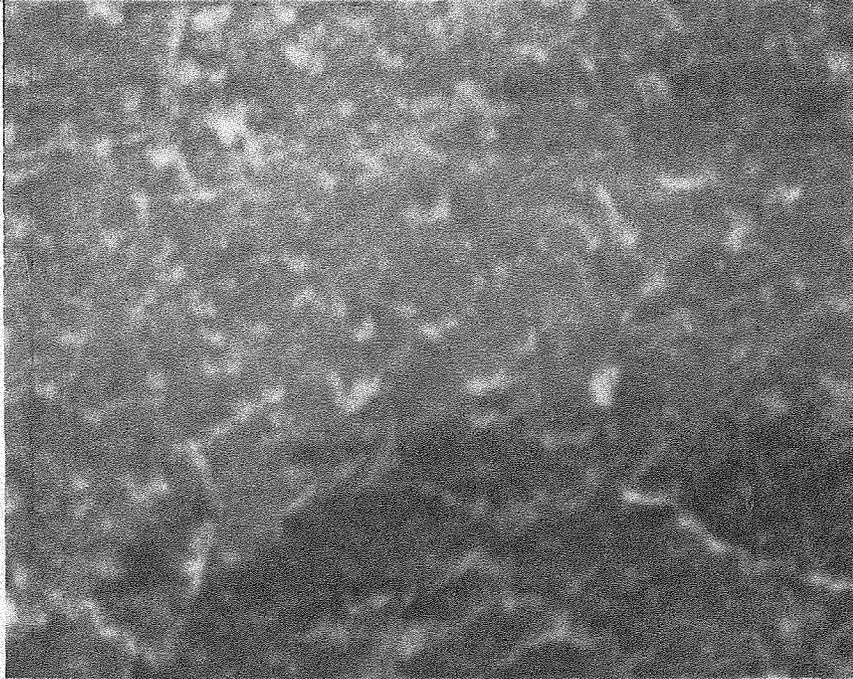
Figure 23   XBB 800-14893
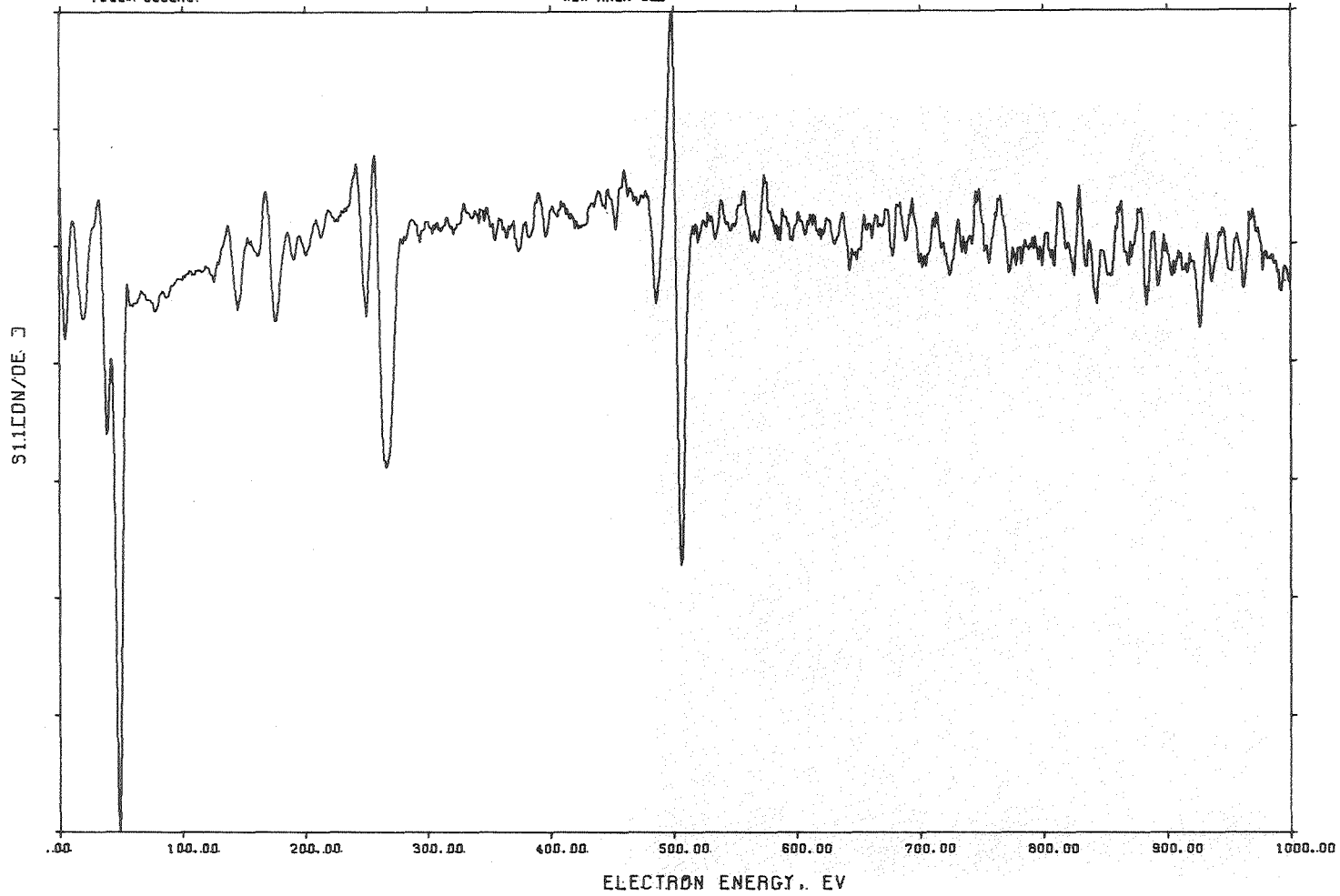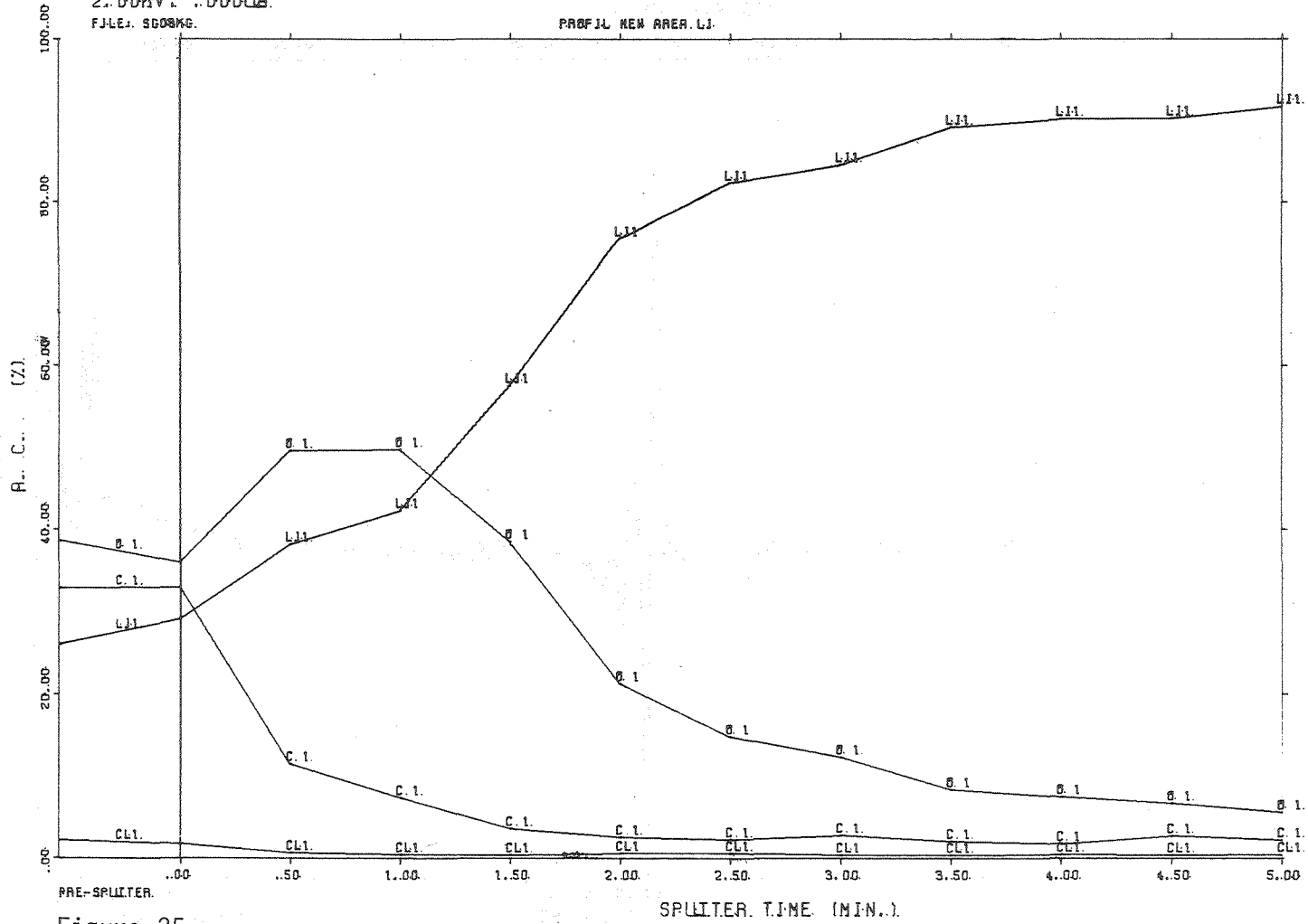
Figure 24

XBL 8012-13566

Figure 25

XBL 8012-13562

Figure 26

XBL 8012-13563

W = 0.6l eV

Figure 27

XBL808-5726